

REPORT DOCUMENTATION PAGE					Form Approved OMB No. 0704-0188	
<p>The public reporting burden for this collection of information is estimated to average 1 hour per response, including the time for reviewing instructions, searching existing data sources, gathering and maintaining the data needed, and completing and reviewing the collection of information. Send comments regarding this burden estimate or any other aspect of this collection of information, including suggestions for reducing the burden, to the Department of Defense, Executive Service Directorate (0704-0188). Respondents should be aware that notwithstanding any other provision of law, no person shall be subject to any penalty for failing to comply with a collection of information if it does not display a currently valid OMB control number.</p> <p><b>PLEASE DO NOT RETURN YOUR FORM TO THE ABOVE ORGANIZATION.</b></p>						
1. REPORT DATE (DD-MM-YYYY) 28-02-2013		2. REPORT TYPE Final		3. DATES COVERED (From - To) 01-02-2008 to 30-11-2012		
4. TITLE AND SUBTITLE Non-Evaporative Cooling via Inelastic Collisions in an Optical Trap				5a. CONTRACT NUMBER FA9550-08-1-0031 P0005		
				5b. GRANT NUMBER		
				5c. PROGRAM ELEMENT NUMBER		
6. AUTHOR(S) Roberts, Jacob L				5d. PROJECT NUMBER		
				5e. TASK NUMBER		
				5f. WORK UNIT NUMBER		
7. PERFORMING ORGANIZATION NAME(S) AND ADDRESS(ES) Colorado State University CSU Office of Sponsored Programs 2002 Campus Delivery, Fort Collins, CO, 80523-2002				8. PERFORMING ORGANIZATION REPORT NUMBER		
9. SPONSORING/MONITORING AGENCY NAME(S) AND ADDRESS(ES) Air Force Office of Scientific Research 875 N. Randolph Street Suite 325, Room 3112 Arlington Virginia, 22203-1954				10. SPONSOR/MONITOR'S ACRONYM(S) DOD-USAF		
				11. SPONSOR/MONITOR'S REPORT NUMBER(S) AFRL-OSR-VA-TR-2013-0160		
12. DISTRIBUTION/AVAILABILITY STATEMENT Distribution A						
13. SUPPLEMENTARY NOTES						
<b>14. ABSTRACT</b> <p>Through the use of spin-exchange collisions in a magnetic field combined with optical pumping, it is possible to cool an ultracold gas without requiring the loss of atoms. This cooling technique was implemented and characterized for 85-Rb and 87-Rb in an optical trap. Unexpected optical trap loading physics during the simultaneous loading of the two Rb isotopes and hyperfine changing collisions that were difficult to avoid without encountering problems with reabsorption of optical pumping photons presented significant challenges to effective cooling in this Rb mixture. A characterization of the cooling was conducted that provided criteria for evaluating systems suited to this cooling technique. The model of the cooling process indicates that the use of two different types of atoms in the cooling as opposed to a single type of atom should show significant benefits as the density of the gas increases. Additional measurements led to the development of an ultracold plasma apparatus that was designed to confine ultracold plasmas in a Penning trap. The ultracold plasmas produced in this apparatus had much lower density than typical systems elsewhere, and that has led to studies of ultracold plasma oscillation, response to short electric field pulses, and electron evaporative cooling.</p>						
<b>15. SUBJECT TERMS</b> <p>Plasma physics; laser cooling and trapping; ultracold atoms; ultracold neutral plasmas; ultracold collisions</p>						
16. SECURITY CLASSIFICATION OF:			17. LIMITATION OF ABSTRACT  UU	18. NUMBER OF PAGES  49	19a. NAME OF RESPONSIBLE PERSON Jacob L Roberts	
a. REPORT  U	b. ABSTRACT  U	c. THIS PAGE  U			19b. TELEPHONE NUMBER (Include area code) 970-491-0578	

Reset

Standard Form 298 (Rev. 8/98)  
Prescribed by ANSI Std. Z39.18  
Adobe Professional 7.0

**Final Technical Report for Research Project**

**FA9550-08-1-0031 P0005**

**“Non-Evaporative Cooling via Inelastic Collisions in an Optical  
Trap”**

**Jacob L. Roberts, Principal Investigator**

**Colorado State University**

**February 28, 2013**

**Reporting Period: Feb. 1, 2008 to Nov. 30, 2012**

## **Abstract**

Through the use of spin-exchange collisions in a magnetic field combined with optical pumping, it is possible to cool an ultracold gas without requiring the loss of atoms. This cooling technique was implemented and characterized for  $^{85}\text{Rb}$  and  $^{87}\text{Rb}$  in an optical trap. Unexpected optical trap loading physics during the simultaneous loading of the two Rb isotopes and hyperfine changing collisions that were difficult to avoid without encountering problems with reabsorption of optical pumping photons presented significant challenges to effective cooling in this Rb mixture. A characterization of the cooling was conducted that provided criteria for evaluating systems suited to this cooling technique. The model of the cooling process indicates that the use of two different types of atoms in the cooling as opposed to a single type of atom should show significant benefits as the density of the gas increases. Additional measurements led to the development of an ultracold plasma apparatus that was designed to confine ultracold plasmas in a Penning trap. The ultracold plasmas produced in this apparatus had much lower density than typical systems elsewhere, and that has led to studies of ultracold plasma oscillation, response to short electric field pulses, and electron evaporative cooling (in progress).

## **I. Executive Summary**

The primary initial goal of this research project was the implementation and evaluation of a novel non-evaporative cooling scheme for ultracold atoms, called Collision-assisted Zeeman cooling [1]. This cooling scheme was implemented and evaluated during the time period associated with this project, but as the research progressed there were opportunities to study physics associated with this main research program that led in unexpected directions. In the end, this led to research concerning not only Collision-assisted Zeeman (CAZ) cooling, but also ultracold plasma physics [2]. This final report details the scientific findings that occurred as part of this project, describes the course of the research and the capabilities that have been developed as a result, and looks towards future projects both with respect to novel non-evaporative cooling and ultracold plasma physics. In the executive summary, a brief description of the major results of this research will be presented. Additional motivation and details will be provided in the main body of the report along with comments on future research directions.

### **I.A Collision-assisted Zeeman Cooling**

CAZ cooling works through a combination of spin-exchange collisions in an external magnetic field and optical pumping [1]. We implemented this cooling scheme in a gas of ultracold  $^{85}\text{Rb}$  and  $^{87}\text{Rb}$  atoms confined in an optical trap. Unlike in the original theoretical proposal of the technique [1], we used two different types of atoms rather than a single type of atom. The generalization of the technique to two different types of atoms is straightforward. Figure 1 shows a description of the implementation of this cooling scheme, which has similarities to nuclear demagnetization cooling [3] and similar ultracold atom cooling techniques [4].

We measured the cooling rate obtained through this technique in our experimental apparatus, and investigated the maximum possible cooling rate we could have obtained ( $10.50 \pm 0.71 \mu\text{K/s}$  in a  $37 \mu\text{K}$  gas) as well as the relevant heating mechanisms that occurred during the optical pumping of the gas ( $4.28 \pm 0.65 \mu\text{K/s}$ ). We found that two aspects of  $^{85/87}\text{Rb}$  presented serious

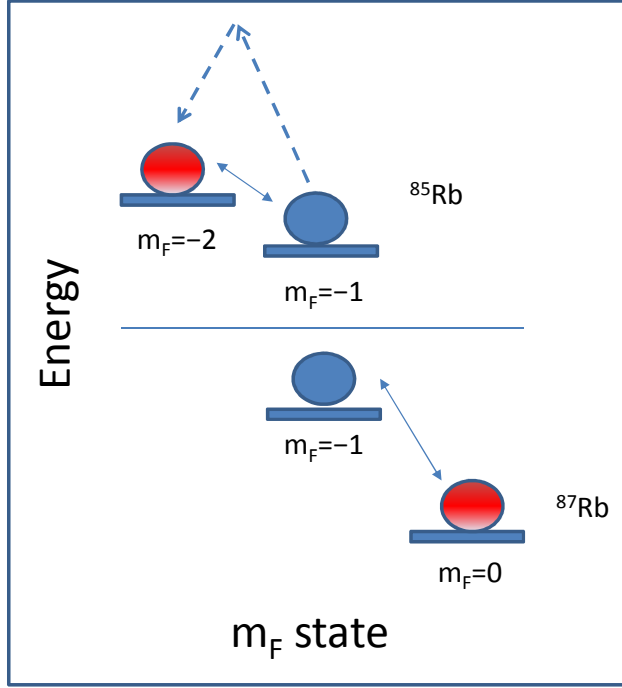


**Figure 1:** Collision-assisted Zeeman (CAZ) cooling in an  $^{85/87}\text{Rb}$  mixture. This figure depicts the cooling cycle associated with CAZ cooling. The red spheres indicate the initial magnetic sublevel ( $m_F$ ) states of  $^{85}\text{Rb}$  and  $^{87}\text{Rb}$ . A magnetic field is present and so there is a Zeeman shift in the energy of these sublevels. A spin-exchange collision (solid arrows) transfers the states from the red spheres to the blue. Because of different  $g_F$  factors, the increase in  $^{87}\text{Rb}$  Zeeman energy is greater than the decrease in  $^{85}\text{Rb}$  Zeeman energy, and so the magnetic energy of the colliding pair increases while the kinetic energy decreases. After the spin-exchange collision has occurred, the  $^{85}\text{Rb}$  atom is optically pumped back to the  $m_F = -2$  state. Periodically, the  $^{87}\text{Rb}$   $m_F$  populations are

scrambled to prevent a buildup of atoms in the  $m_F = -1$  state. Thus, the atoms eventually return to their initial magnetic sublevel, but with less kinetic energy.

challenges in effectively implementing this cooling technique: the two isotopes of Rb interfered with each other during optical trap loading in a way that compromised the initial conditions for the start of cooling; and hyperfine-changing collisions appear to present a serious limitation whose solution would require introducing undesirable reabsorption into the optical pumping process [5,6].

We developed a simple analytic expression to describe this cooling technique:

$$\frac{dT}{dt} = -\frac{1}{\tau_{SE}} \frac{\exp\left(\frac{-\Delta}{k_B T}\right) N_2}{3k_B (N_1 + N_2)} (\Delta - \kappa) \frac{1}{1 + \tau_{OP} / \tau_{SE} \left(1 + \exp\left(\frac{-\Delta}{k_B T}\right)\right)} \quad (1)$$

where  $T$  is the temperature of the ultracold gas,  $\tau_{SE}$  is the spin-exchange collision time,  $\Delta$  is the amount of kinetic energy converted to Zeeman energy in a spin-exchange collision,  $\kappa$  is the heat imparted per successful optical pumping cycle,  $k_B$  is Boltzmann's constant,  $\tau_{OP}$  is the

characteristic optical pumping time,  $N_1$  is the number of non-optically pumped atoms, and  $N_2$  is the number of optically pumped atoms. We confirmed that this equation's predicted cooling rate matched our observations. In the manuscript listed below, we detail possible solutions to the difficulties that we encountered in our implementation of this technique and discuss how in principle the use of two different types of atoms for non-evaporative cooling should bring significant increases in cooling rate under reabsorption-limited conditions.

*Publication (submitted):* R. C. Ferrier, M. S. Hamilton, and J. L. Roberts, *Collision-assisted Zeeman Cooling with Multiple Types of Atoms*, submitted to Journal of Physics B (2013), arXiv:1302.5035 (2013).

*Graduate thesis describing the apparatus and the cooling technique:* Anthony R. Gorges, *Simultaneous trapping of  $^{85}\text{Rb}$  &  $^{87}\text{Rb}$  in a far-off-resonance optical trap*, Ph. D. Thesis, Colorado State University (2010).

[http://digitool.library.colostate.edu/R/?func=dbin-jump-full&object\\_id=87604&local\\_base=GEN01](http://digitool.library.colostate.edu/R/?func=dbin-jump-full&object_id=87604&local_base=GEN01)

## **I.B Simultaneous loading of $^{85}\text{Rb}$ and $^{87}\text{Rb}$ into an optical trap from a Magneto-optic Trap (MOT)**

As was mentioned in the previous section, when both stable isotopes of Rb were loaded into an optical trap simultaneously from a MOT they exhibited unexpected cross-isotope interference. We investigated this optical trap loading in detail, measuring the relevant light-assisted collisions, characterizing the cross-isotope load rate interference, and developing a model of the loading process. The cross-isotope interference was identified as originating from dipole-dipole interactions between colliding atoms, induced by off-resonant laser light in the case of one of the atoms in the colliding pair. Despite the laser detunings of several hundred natural linewidths, estimates showed that a large enough dipole was still induced in the atoms to result in a sufficient collision rate to disrupt the optical molasses cooling that was vital for effective loading of the optical trap [7]. This work indicated the presence of unexpected density-dependent effects in laser cooling.

*Publication: M. S. Hamilton, A. R. Gorges, and J. L. Roberts, Inter-isotope effects in optimal dual-isotope loading into a shallow optical trap, Journal of Physics B, **45**, 095302 (2012)*

### **I.C Enhanced light-assisted collisional loss in a two-color MOT**

Because our implementation of CAZ cooling required the creation of two MOTs that overlapped the same region in space, we could easily investigate the effect of illuminating a Rb MOT with light that coupled the first excited state (5P) that was used in the laser cooling to a more highly excited state (5D). We found a substantial increase in the density-dependent loss from the MOT when this was done. Through conducting a series of measurements, we were able to identify the loss channel and determine an explanation for the enhanced loss. The additional laser promoted colliding atoms from the 5S-5P molecular state to the longer-lived 5S-5D molecular state. The atoms had acquired an acceleration towards one another while on the 5S-5P molecular potential, however, and in the longer-lived 5S-5D state the atoms could approach each other much more closely leading to either state-changing collision or radiative escape via a spontaneous decay to the 5S-5P molecular state.

These measurements are relevant for ultracold atom experiments involving excitations to higher excited states than the first excited state [8,9,10] and for evaluating the feasibility of such experiments in Rb.

*Publication: T. M. Wilson and J. L. Roberts, Enhanced light-assisted-collision rate via excitation to the long-lived  $5S_{1/2}$ - $5D_{5/2}$  molecular potential in an  $^{85}\text{Rb}$  magneto-optical trap, Phys. Rev. A **83**, 033419 (2011)*

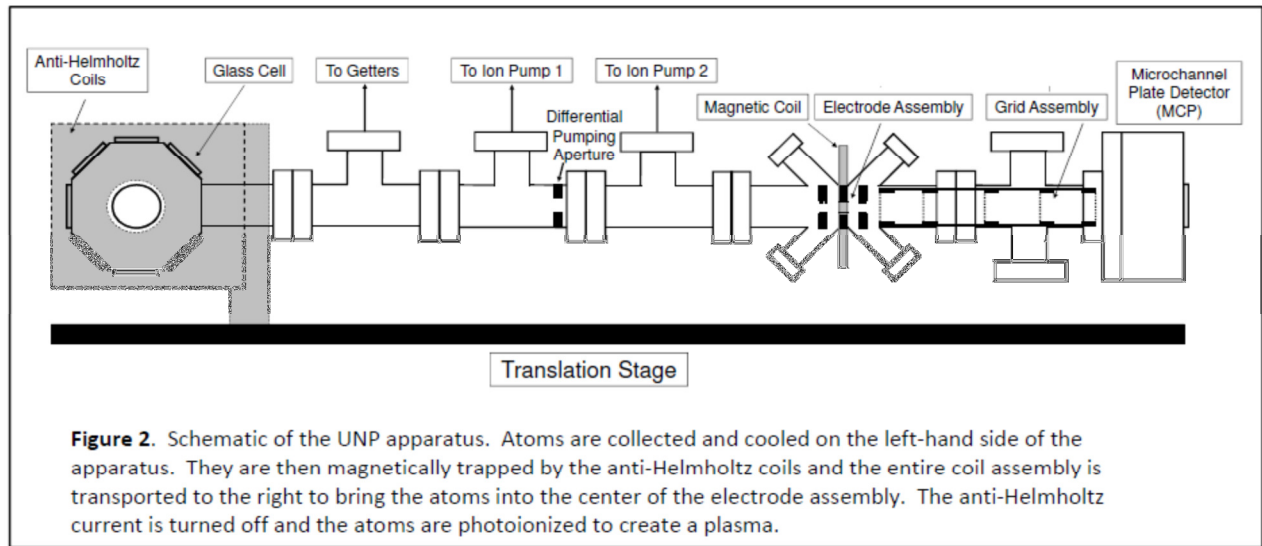
### **I.D Ultracold plasma response to few-cycle rf pulses**

As will be detailed in the main body of the report given below, the experiment described in the previous section led us to consider ultracold plasma research directions that ultimately resulted in the construction of a new ultracold plasma apparatus (supported via a DURIP award FA9550-09-1-0385). The details of the apparatus can be found in the publication listed below and in section VI. The apparatus is designed to confine ultracold plasmas (UCPs) in a Penning trap to extend their lifetime. This will allow the study of longer-timescale processes that cannot be accessed in non-trapped UCP systems.

As a result of the apparatus design, the UCPs that are produced in our system have a much lower density ( $\sim 10^7$ - $10^8 \text{ cm}^{-3}$ ) than is typical in other UCP experiments. We have found that this

lower density has many unexpected benefits and alters the behavior of the UCPs in significant ways. One of the consequences of lower density is that the timescale associated with collisional damping lengthens, allowing oscillatory behavior to persist at lower density where it quickly damped away at higher density.

One of the fundamental collective oscillations in any plasma is a plasma oscillation. Because the plasma oscillation frequency is density-dependent, the response of UCPs to frequencies near the expected plasma oscillation frequency can be used as a probe of the UCP density and thus size. For typical UCPs, the plasma oscillation frequency is in the rf range. We measured the response of the UCPs in our apparatus to very short (as short as only two cycles) rf pulses. Because the pulses were so short, we could clearly measure the delay in time between the application of the pulse and the response of the UCP.



Our observations did not accord with the usual picture of UCP response to applied rf fields [11,12,13]. The response we observed was much too fast for our UCP conditions to be the result of electron heating brought about by local excitation of electron motion. Additionally, our observed response did not scale as a collision-based response would with UCP density or temperature.

Through additional observations, we identified the UCP response in our system as being due to the rf field displacing the electron component of the UCP as a whole with respect to the ions. This displacement produces electric fields that are strong enough to impart enough



acceleration to high-energy electrons in the thermal distribution to drive them from the UCP. As a consequence, while we observed a density-dependent response the resonant frequency was different than that predicted by the standard UCP theory that was based on a different set of UCP parameters than what we have in our apparatus. We were able to develop a model that predicted the UCP resonant frequency, and observed that the model predicted the frequency consistently over numerous UCP parameters.

In the absence of this measurement, we would not have been able to extract densities accurately from our system, complicating the interpretation of almost any UCP experiment we would perform. Thus, not only is this measurement interesting in its own right, it was also necessary in order to perform future measurements effectively in our apparatus.

*Publication: Truman M. Wilson, Wei-Ting Chen, and Jacob L. Roberts, Density-dependent response of an ultracold plasma to few-cycle radio-frequency pulses, Phys. Rev. A **87**, 013410 (2013).*

## **I.E List of students**

Graduate students:

Anthony Gorges, Ph. D. (2010)  
Mathew Hamilton, anticipated Ph.D. (2013)  
Truman Wilson, anticipated Ph.D. (2013)  
Rebekah Ferrier, anticipated Ph.D. (2013)  
Wei-Ting Chen, anticipated Ph.D. (2014)  
Craig Witte, anticipated Ph.D. (2016)

Undergraduate Students:

Samantha Mitchell  
Matthew Heine  
Daniel Illenberger  
Andrew Davis

This concludes the executive summary section of this report.

Table of Contents

II. Collision-assisted Zeeman Cooling: Background and Context .....	11
III. Simultaneous loading of $^{85}\text{Rb}$ and $^{87}\text{Rb}$ into an optical trap .....	15
IV. Collision-assisted Zeeman Cooling with Multiple Types of Atoms .....	20
IV.A Single-type-of-atom CAZ cooling .....	20
IV.B Multiple-type-of-atom CAZ cooling .....	21
IV.C Analytic prediction for 2-CAZ cooling rate .....	23
IV.D Experimental Measurements .....	24
IV.E Implications for Effective 2-CAZ Cooling .....	27
IV.F Multiple- vs. single-type-of-atom cooling .....	28
V. Enhanced two-color light-assisted collisional losses in Rb MOT .....	30
VI. A trap for ultracold neutral plasmas .....	33
VI.A Axial confinement of UCPs in a Penning trap .....	35
VI.B UCP density-dependent response to few-cycle rf pulses .....	37
VII. Investigations started during the reporting period, still in progress, and future work. ....	41
VII.A Evaporative cooling in ultracold plasmas .....	41
VII.B Magnetic field influence on initial ultracold plasma expansion rate .....	42
VII.C Ultracold plasma damping rate .....	43
VII.D Spin-exchange collision rate measurement .....	44
VII.E Spatially-selective Hyperfine Pump Cooling .....	44
VIII. Conclusion .....	46

## II. Collision-assisted Zeeman Cooling: Background and Context

The laser cooling technique that is in most common use today is Doppler cooling [14,15,16], followed closely by optical molasses cooling [17,18] with atoms for which it is feasible. Remarkably, these laser cooling techniques were those used in the initial research into laser cooling of neutral atoms in the 1980s, and they have proven to be effective and robust in a wide variety of applications. For both of these techniques, however, there is a lower limit to the temperature to which the atoms can be cooled. While many experiments can be conducted with atoms above these limiting temperatures, there are many others that require colder temperatures than the Doppler limit and optical molasses cooling limits will allow. In particular, for the creation of Bose-Einstein condensates [19,20] and Fermi-degenerate gases [21], further cooling below these laser cooling limits is required.

The most common way to perform this additional cooling is through the use of forced evaporative cooling [22,23]. Evaporative cooling has proven itself to be effective and robust in a wide variety of ultracold atomic gases. However, it does have drawbacks. First, for typical experimental conditions evaporative cooling requires the loss of most of the initially trapped gas in order to reach the temperatures of interest. For systems where enough atoms can be obtained at the start of evaporative cooling, experiments can still be conducted by loading far more atoms than are ultimately needed. For systems where the initial number of atoms is limited, then evaporative cooling just those atoms alone will not generally result in samples large enough to perform desired measurements.

Beyond the atom loss, the use of evaporative cooling in all but magnetic traps generally requires the modification of the trap geometry in order to let the highest-energy atoms escape from the gas to perform the cooling. This becomes problematic if the goal is to use confining potentials that are not the usual harmonic-oscillator-like ones. More flexibility can be gained if the potential is not linked directly to the cooling method. Evaporative cooling usually requires a segmentation of the vacuum system into an initial laser cooling and ultracold atom collection region and an evaporative cooling and science region [24]. A faster cooling technique eliminates this experimental complexity. Finally, there is intrinsic physics interest in

investigating the ways that an ultracold gas can be cooled, and robust cooling techniques could be useful in the development of technological applications that require very cold ultracold gases.

Because of this interest in non-evaporative cooling, non-evaporative cooling techniques [25,26,27] have been investigated both experimentally and theoretically. Many of these involve extensions to laser cooling beyond Doppler and optical molasses cooling. While many of laser cooling extension techniques have been successful for ultracold gases with relatively low density, increasing the density of the gas being cooled to more useful levels resulted in a degradation of the cooling efficiency due to the increasing optical thickness of the gas. The reason for this is that cooling anything requires the removal of entropy. For light-based cooling techniques, this means that photons must be able to escape the gas in order for the cooling to work. For an optically thick gas, the photons that need to escape scatter repeatedly before leaving the gas, resulting in unwanted heating and usually a disruption of the cooling technique being used.

In addition to these extensions of laser cooling techniques, there have been techniques that exploit the spin structure and spin-changing collisions of some ultracold atoms to use collisions to cool a gas in a magnetic field. In the work of Ref. [28], spin-exchange collisions are used in a method that results in a one-time reduction of the temperature of the gas. Much closer to the research described in this final report, dipole relaxation collisions in  $^{52}\text{Cr}$  in a magnetic field have been used in a technique reminiscent of nuclear (and electronic) demagnetization cooling to create a closed cooling cycle that does not require the loss of atoms from the gas. In fact, the main difference between the work in Ref. [4] and one-component CAZ cooling is the use dipole relaxation rather than spin-exchange collisions in the cooling cycle.

CAZ cooling consists of using a combination of spin-exchange collisions in an externally applied magnetic field and optical pumping to cool an ultracold gas in a closed cooling cycle that does not require the loss of any atoms from the gas. While the precise details of the cooling are described in more detail below, the general idea is to spin-polarize the atoms into particular spin states so that any spin-exchange collisions that change the atoms' spin states will result in

an increase in the Zeeman energy of the colliding atom pair. This increase of energy comes from the kinetic energy of the atoms in the spin-exchange collision, and so effectively kinetic energy is transferred to magnetic potential energy. After the spin-exchange collisions have been given time to occur, the atoms are optically pumped back into their initial states. Thus, the atoms return to their initial spin states, but have less kinetic energy. Hence, the gas has been cooled. The entropy that is removed from the gas is carried away by the photons scattered during optical pumping.

This cooling scheme was first proposed theoretically in Ref. [1]. In that original proposal, the theoretical treatment was performed assuming one type of atom was present in the gas being cooled. In this work, however, two types of atoms were used. This requires a straightforward extension of the theoretical description of the cooling technique, but has multiple advantages. First, it is possible to search for a pair of atoms that has particularly favorable spin-exchange collision rates. Second, as will be described in more detail below, atoms can be used that require the first-order Zeeman effect rather than second-order Zeeman effect for cooling, resulting in easier experimental apparatus design. The use of two atoms rather than one increases the range of the applicability of the Collision-assisted Zeeman cooling technique: in the original conception of the cooling an atom with hyperfine structure had to be used. In the extension to this original theory, the only requirement is that the atoms have a non-zero electronic spin in their ground state, and that the two atoms have a different  $g$ -factor associated with the Zeeman shift. Finally, there are predicted to be significant advantages of using two different types of atoms with regard to mitigating the effect of reabsorption: one of the two types of atoms can be kept optically thin while the other can maintain a higher density that is often required for useful experiments. The details of this predicted reabsorption mitigation are also presented below.

For both the single- and two-type-of-atom Collision-assisted Zeeman cooling techniques, there are several potential advantages. The spin-exchange collisions happen spontaneously. The main experimental control is a magnetic field, which is generally easy to apply and change. The cooling technique is naturally three-dimensional. In contrast to non-evaporative cooling

techniques where the energy removed per optical pumping photon is approximately proportional to the gas temperature ( $T$ ) as  $T^{1/2}$ , the energy carried away in this collision-based cooling technique is proportional to  $T$ . This means that at temperatures well above those associated with the photon recoil limit, more energy can be removed per optical pumping photon in this collision-based technique. Again, for situations where optical thickness and reabsorption is an issue, this is advantageous.

Unfortunately, there are disadvantages as well. Spin-exchange collisions are slower than the rate at which photons are scattered for typical conditions, and so the achievable cooling rate is potentially too slow. This places a premium on the initial conditions (density and temperature) that can be obtained for the gas being cooled. In a slightly related note, since inelastic collisions are at the heart of the cooling scheme it must be possible for the atoms in the gas to collide inelastically. This means that there is the possibility of unwanted loss-inducing collisions that can occur in the gas, too. Disappointingly, both of these factors placed a severe limitation on the cooling that we were able to achieve in our experimental system.

This being said, we were able to demonstrate the cooling and we successfully characterized the achieved cooling rate and the relevant loss and heating rates in our system. We were able to develop a simple analytic model that describes the predicted cooling rate and then confirmed the predictions of that model experimentally. This agreement indicates that the model can be used to analyze the performance limitations accurately to determine how to ultimately achieve better cooling behavior. This characterization improves the understanding of the performance of the cooling in an actual experimental system, and points the way towards the necessary requirements for efficiently implementing this cooling technique. Most likely, a different set of atom types would likely be required.

There are reasons in general to pursue this line of investigation concerning Collision-assisted Zeeman cooling despite the difficulties encountered in our measurements. The heating mechanisms and initial condition restrictions are associated with the Rb mixture that we used and could be avoided in other systems with different atoms. Even with the Rb mixture, there are simple techniques that can be used to improve the initial conditions for the cooling.

Collision-assisted Zeeman cooling is insensitive to the details of the confining potential for the atoms and so it could be used to load traps that have non-standard trapping potentials (e.g. potentials steeper than harmonic traps approximating square well potentials; ring or racetrack potentials with topological features). And, while reabsorption in an optically thick gas was not ultimately a difficulty in our system, the use of two different types of atoms still holds significant promise for increasing the effective cooling rate in situations where reabsorption is a limiting factor. The details behind this reabsorption mitigation will be presented in the appropriate subsection below.

### III. Simultaneous loading of $^{85}\text{Rb}$ and $^{87}\text{Rb}$ into an optical trap

*Publication:* M. S. Hamilton, A. R. Gorges, and J. L. Roberts, *Inter-isotope effects in optimal dual-isotope loading into a shallow optical trap*, *Journal of Physics B*, **45**, 095302 (2012)

All of the measurements that we conducted concerning Collision-assisted Zeeman (CAZ) cooling were performed with a mixture of  $^{85}\text{Rb}$  and  $^{87}\text{Rb}$  loaded into a far off-resonance optical trap (FORT). There were several reasons for choosing this pair of atoms for our measurements. Our laser systems could be adapted to either isotope, leading to flexibility in our apparatus design and experimentation. The laser systems required for Rb laser cooling and optical pumping are inexpensive and well-known. Finally, there is a relatively large spin-exchange collision rate between  $^{85}\text{Rb}$  and  $^{87}\text{Rb}$ .

To explore CAZ cooling,  $^{85}\text{Rb}$  and  $^{87}\text{Rb}$  atoms had to be confined to an optical trap. Initially, ultracold atoms of each isotope were cooled into overlapping Magneto-optic Traps (MOTs). From there, the atoms were then loaded into a Far-off-resonance optical trap (FORT). The loading of one type of ultracold atom into a FORT has been studied in detail [29,30] and more than one type of atom had been loaded into an optical trap previously [31,32], but the loading dynamics of the multiple-atom optical traps had not been studied in detail. In any case, there were no previous reported studies on the physics associated with simultaneously loading  $^{85}\text{Rb}$  and  $^{87}\text{Rb}$  into an optical trap.

Our experimental goal was to have the highest densities of  $^{85}\text{Rb}$  and  $^{87}\text{Rb}$  possible for the best initial spin-exchange collision rate (and thus largest cooling rate) for our planned measurements. To that end, the FORT parameters were set to produce the largest number of trapped atoms for a given effective trap volume. As part of this optimization, we found that larger-volume but therefore shallower optical traps resulted in a better performance. The optical trap that we used confined the atoms in a conservative potential. Thus, trapping the atoms that entered the optical trap from outside it required cooling them to remove energy. Shallow traps result in increased cooling requirements since the ultimate temperature of the trapped gas is lower.

Ideally, the two isotopes would not impact each the other's loading at all and the total number of atoms that could be loaded simultaneously would be the sum of the number of atoms that were loaded individually. One deviation from this ideal case occurs through the fact that the use of near-resonant laser light during optical trap causes cross-isotope light-assisted collisions [33,34] that will result in loss, reducing the simultaneously trapped atom number. These loss rates are extremely difficult to calculate for atoms with hyperfine structure from first principles, and so we measured the applicable rates explicitly.

We combined this explicit measurement of the cross-isotope loss rates with a measurement of the individual isotopes' loading rates from the MOT to the optical trap. In principle this should have yielded an accurate prediction of the total number of atoms that could be confined in the optical trap during simultaneous loading of  $^{85}\text{Rb}$  and  $^{87}\text{Rb}$ . However, our observations of the total number of atoms trapped produced numbers that were far lower than predicted on the basis of these measured loading and loss rates.

Additional study found that not only did the presence of another isotope result in loss through cross-isotope collisions, but the loading rate of atoms from the MOT to the optical trap was adversely affected as well. We were able to observe this phenomenon directly by measuring the optical trap loading rate of  $^{87}\text{Rb}$  both with and without the presence of  $^{85}\text{Rb}$  atoms. The only laser light present during these experiments was the light associated with  $^{87}\text{Rb}$  transitions and thus the  $^{85}\text{Rb}$  atoms were "dark." Thus, these results were somewhat surprising as the off-



resonant scattering rates of  $^{85}\text{Rb}$  in  $^{87}\text{Rb}$ -resonant light were on the order of one photon in the entire time of the experimental sequence. Light-assisted collision losses could be ruled out on the basis of the measured rates and densities of the gases in the experiments.

We performed additional experiments in order to investigate this phenomenon and found that the presence of  $^{85}\text{Rb}$  atoms changed the  $^{87}\text{Rb}$  hyperfine steady-state populations in the light used in the loading sequence. Again, all known collision rates were insufficient to account for such an effect, similar to the observed loading rate reduction. Thus, we needed to determine how such effects could occur despite the inter-isotope difference in resonant frequency.

A full model of the collision between an  $^{85}\text{Rb}$  and  $^{87}\text{Rb}$  atom in the presence of laser light in a laser cooling configuration is beyond the capability of current atomic theory [35]. The primary difficulty is that the hyperfine structure of the two Rb isotopes means that there are about 500 states that are relevant to the collision and spherical symmetry is broken because the laser polarization direction is relevant.

Instead, we modeled the influence of the laser light on the interatomic potentials by calculating dressed ground states even with the wide variety of states that were potentially involved in the collision, in a simplified treatment of the full version of the treatment described in [36]. The result of such a calculation is shown in figure 2. The calculation was performed by creating a matrix that included the energy of all of the ground-state/ground-state pairs and excited-state/ground-state pairs along the diagonal in a dressed state treatment that accounted for the photon energy of the light. The light coupling was included in the appropriate off-diagonal elements for states which the light coupled together, given an assumed polarization. The long-range atom-atom interaction for a particular radius  $R$  was included in the off-diagonal matrix elements as well [37] assuming a particular collision direction. The entire matrix was diagonalized to find the energies of the now-dressed ground-state/ground-state atom pairs (i.e. the atoms are no longer purely in the ground state due to the dressing field).

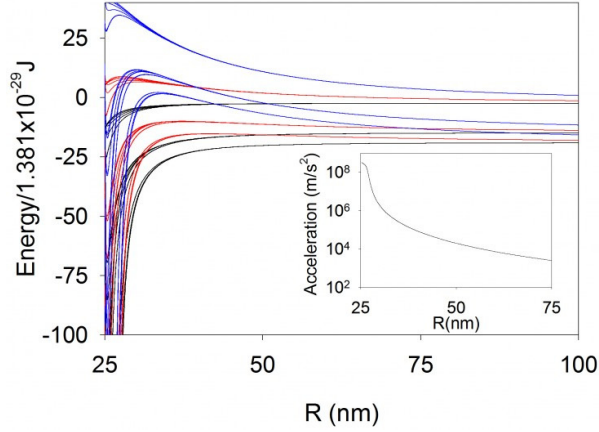


**Figure 2.** Dressed ground state potentials including the induced dipole-dipole interaction between the  $^{87}\text{Rb}$   $F=2$  ground state and the  $^{85}\text{Rb}$   $F=2$  ground state for our  $^{87}\text{Rb}$  a set of cooling light parameter that matched our experimental conditions: intensity of  $36 \text{ mW/cm}^2$ , assumed linear polarization, semi-classical collision direction along the polarization direction, and detuning of 120 MHz to the red of the  $^{87}\text{Rb}$  cycling transition. The large number of potential curves comes from the many possible combinations of  $mF$  states for both  $^{85}\text{Rb}$  and  $^{87}\text{Rb}$ . Potentials for s-wave (black), p-wave (red), and d-wave (blue) collision channels are shown. The

potentials have significant curvature even at long range and are state-dependent as well. The inset shows the center-of-mass acceleration associated with the steepest s-wave potential on a log scale.

We found that despite the  $^{87}\text{Rb}$ -resonant laser light's detuning from the  $^{85}\text{Rb}$  resonances by several hundred natural linewidths, the dipole-dipole interaction induced by the laser light between two colliding  $^{85}\text{Rb}$  and  $^{87}\text{Rb}$  atoms was significant on the scale of ultracold collisions even at relatively large radii. Collision channels that would normally be closed were opened due to the induced dipole-dipole interaction. The light-induced interaction was strong enough to create state-dependent scattering amplitudes that were significant for the range of collision energies that were encountered during the loading of the optical trap.

Since the trap was shallow ( $120 \mu\text{K}$  deep in these experiments), Doppler cooling was insufficient to load the optical trap. Instead, optical molasses was required. Optical molasses relies on coherences between the spin states of the atoms being cooled in order to be effective [38] and so a significant collision rate can disrupt the cooling. This would be manifested in a lower collisional rate and changes in the hyperfine state distribution, as observed in our measurements.

Our work in the publication cited at the start of this section provides detailed loading rates, light-assisted collision rates for both cross-species and intra-species collisions, measurements of the loading rate reduction and the change in hyperfine state distribution, and model of the optical trap loading process.

This work had specific implications for CAZ cooling in the  $^{85/87}\text{Rb}$  system, as well as more general implications. The specific implication is that the simultaneous loading of both isotopes of Rb would not be nearly effective as would be extrapolated from the loading performance of each individual isotope. The number of atoms that could successfully be loaded into the optical trap was thus significantly lower than our initial expectations. Moreover, the interference between the two isotopes had implications for the reproducibility of our measurements. Small drifts in the system that produce small changes for single-isotope optical trap loading are magnified in their importance for two-isotope optical trap loading. This is because a system drift that results in lower optical trap loading efficiency for one isotope will not only cause a reduction in number for that isotope, but will result in an increase in number of the other isotope. That increase in number will further diminish the number loaded of the first isotope, which in turn feeds back in such a way that small drifts have disproportionate impacts on the ratio of the number of atoms loaded into the optical trap. The cross-isotope light-assisted collisions are largely responsible for this effect, but the load rate reduction plays a role as well.

The general implications of this work are that the degradation in optical molasses cooling efficiency associated with the increase in density of the atom being cooled also extends to the density of other atoms in the gas, despite large detuning differences between the two atoms. This effect will be most pronounced for different isotopes of the same element, but will also occur between different atomic elements entirely. In that case, the detunings will be much larger and thus the induced dipole moments much smaller, mitigating the expected cooling efficiency reduction. However, because of the steep dependence of the intermolecular potential energy with internuclear distance between a colliding pair of atoms, the reduction in the induced dipole moment only reduces the range of dipole-dipole interaction influence – it does not eliminate it.

The specific implications for this physics will be discussed more in the context of the requirements for CAZ cooling in section IV.D below.

## IV. Collision-assisted Zeeman Cooling with Multiple Types of Atoms

*Publication:* R. C. Ferrier, M. S. Hamilton, and J. L. Roberts, *Collision-assisted Zeeman Cooling with Multiple Types of Atoms*, submitted to Journal of Physics B (2013), arXiv:1302.5035 (2013).

### IV.A Single-type-of-atom CAZ cooling

While our experimental implementation of CAZ cooling is not the same as in Ref. [1] since we use multiple types of atoms at the same time rather than just one, it is useful to review the single-type-of-atom cooling since the multiple-atom-cooling is a straightforward extension.

In order to be able to discuss the CAZ cooling technique concretely, I will present the cooling technique for atoms with a specific hyperfine ground state structure. Consider an atom ground state electron orbital angular momentum  $L=0$ , electron spin  $S=1/2$ , and nuclear spin  $I=3/2$  in its  $F=L+S+I=1$  ground state (e.g.  $^{87}\text{Rb}$ ). In an externally applied magnetic field, the Zeeman energy of the atom will depend on the total angular momentum projection quantum number  $m_F$  along the direction of the externally applied magnetic field. The largest part of the shift is due to the linear Zeeman shift. However, there is also a second-order Zeeman shift so that the total energy shift to second-order is equal to

$$\Delta E_{Zeeman} = -\frac{\mu_B B}{2} m_F - \frac{(\mu_B B)^2}{\hbar \omega_F} \left(1 - \frac{m_F^2}{4}\right) \quad (2)$$

where  $\mu_B$  is equal to the electron Bohr magneton,  $B$  is the magnitude of the externally applied magnetic field, and  $\hbar \omega_F$  is equal to the energy difference between the  $F=1$  and  $F=2$  ground hyperfine states.

As a consequence of the second-order shift, the average value of the Zeeman energy of two  $m_F=0$  atoms is less than the average of an  $m_F=+1$  and  $m_F=-1$  atom, and this point is exploited in the cooling scheme. Using optical pumping, the atoms in the gas are optically pumped into the  $F=1$ ,  $m_F=0$  state. This is generally accomplished by applying light linearly polarized along the magnetic field axis and resonant with the  $nS_{1/2} F=1$  to  $nP_{3/2} F'=1$  transition. Since the Clebsch-Gordan coefficient the  $m_F=0$  to  $m_F'=0$  transition in this case is equal to zero, atoms will

accumulate in the  $F=1$   $m_F=0$  state as desired since they cannot be excited by the laser out of it. In addition to the laser already mentioned, a second is required that is resonant with the  $nS_{1/2}$   $F=2$  to  $nP_{3/2}$   $F=2$  transition to prevent atoms from accumulating in the upper hyperfine state during the optical pumping. This laser can be linearly polarized along an axis perpendicular to the applied magnetic field.

Besides the Zeeman shift and the optical pumping, the last thing that is required in the cooling scheme is spin-exchange collisions. These collisions arise because of exchange effects at close range in during a collision and result in change in the individual  $m_F$  states of the colliding pair but preserve the  $m_F$  state sum of the pair. Thus, in the specific example being considered here, two  $m_F=0$  atoms can undergo a spin-exchange collision and emerge as an  $m_F=+1$  and  $m_F=-1$  atom, and vice versa.

A CAZ cooling cycle consists of spin-polarizing the atoms in the gas into the  $m_F=0$  state via optical pumping. An external magnetic field is applied. Spin-exchange collisions between  $m_F=0$  atom pairs will result in an increase in total Zeeman energy for the two atoms through the second-order Zeeman effect. This energy is supplied by the atoms' kinetic energy in the collision. After the spin-exchange collisions have been given time to occur, the atoms are optical pumped back into their original  $m_F=0$  states. Thus, the atoms have returned to their initial  $m_F$  state population, but have reduced kinetic energy. In effect, the spin-exchange collisions transfer kinetic energy to Zeeman energy that is subsequently removed from the gas via optical pumping, forming a closed cooling cycle that cools the gas without requiring the loss of atoms. Entropy is removed during the cooling by spontaneously scattered photons during the optical pumping process.

#### **IV.B Multiple-type-of-atom CAZ cooling**

The extension of CAZ cooling to gases with two types of atoms simultaneously present is straightforward. The same general idea applies: spin-exchange collisions transfer kinetic energy to Zeeman energy that is then removed from the gas via optical pumping. In this case, however, the spin-exchange collisions occur between the two different types of atoms.

Once again, in order to discuss the details of the two-type-of-atom CAZ (2-CAZ) cooling a specific example will be considered that involves atoms with the hyperfine structure of  $^{85}\text{Rb}$  and  $^{87}\text{Rb}$ . The atoms in the example have  $I=5/2, L=0, S=1/2$  and  $I=3/2, L=0, S=1/2$  and are in their  $F=2$  and  $F=1$  lower hyperfine ground states, respectively. Figure 1 in the executive summary shows the nature of the 2-CAZ cooling cycle in this instance. The  $I=5/2$  (i.e.  $^{85}\text{Rb}$ ) atoms are optically pumped into their  $F=2, m_F=-2$  state. They can then collide with  $^{87}\text{Rb}$  atoms in their  $m_F=0$  or  $m_F=+1$  states. Because of the different spins, the g-factors of the two different types of atoms are not the same. Thus, a spin-exchange collision between the  $I=5/2, m_F=-2$  atom and an  $I=3/2, m_F=0$  atom would result in the two atoms each being scattered into their  $m_F=-1$  states and would increase the Zeeman energy of the atom pair by  $\mu_B B/6$ . The kinetic energy of the pair would then decrease by the same amount.

After the spin-exchange collision, the  $I=5/2$  atom is optically pumped back into its  $m_F=-2$  state. The  $I=3/2$  atom  $m_F$  state populations are periodically scrambled via rf sweeps so that the population does not accumulate in any one of the states in particular. Thus, the spin-exchange collisions can occur again, but with kinetic energy having been removed as part of the cooling cycle.

The main disadvantage of this 2-CAZ vs. CAZ is the additional experimental complexity that comes from laser cooling and trapping two different types of atoms rather than one. However, there are many offsetting advantages. For atoms with different g-factors, the energy converted in the spin-exchange collision occurs through the first- rather than second-order Zeeman effect. This means that for typical optical trap parameters, magnetic fields of a few gauss vs. several tens of gauss are required for 2-CAZ vs. CAZ. Not only are these fields easier to produce experimentally, but optical pumping is more difficult to implement for the larger magnetic fields because the Zeeman shifts in the excited states of typical atoms (e.g. alkali atoms) are on the order of the hyperfine splitting of these states and so the various F states of the excited energy levels are thoroughly mixed, complicating the required optical pumping. More importantly, the higher magnetic field in CAZ vs. 2-CAZ results in more heating from non-spin-exchange collisions that change  $m_F$  states such as dipole relaxation collisions. While dipole

relaxation collisions occur much more slowly in general than the spin-exchange collisions, the energy released in these collisions generally scales with the first-order Zeeman shift. Thus, while these undesirable collisions release about the same amount of energy as heat as a typical cooling cycle removes in 2-CAZ, in CAZ cooling they release a factor of 10 or more energy as heat as what is removed in a typical cooling cycle. From the perspective of mitigating the effect of these unwanted collisions, 2-CAZ is far more desirable.

There are other advantages besides the magnetic field scaling as well. In 2-CAZ there are more possibilities for finding a pair of atoms with a favorable spin-exchange rate. Also, one component of the gas in 2-CAZ can have a large number to maintain a high overall density of the gas while the other component can be kept optically thin. This mitigates the problem of reabsorption in the gas.

#### **IV.C Analytic prediction for 2-CAZ cooling rate**

Despite the number of  $m_F$  states that are potentially present in spin-exchange collisions in a gas of  $^{85}\text{Rb}$  and  $^{87}\text{Rb}$ , it is possible to formulate an analytic expression for the predicted 2-CAZ cooling rate. There are several assumptions that go into this expression, but they all reasonable for the  $^{85/87}\text{Rb}$  mixture that was used in our experiments and for other likely combinations of other atoms. The assumptions are that the spin-exchange rate does not vary widely over the range of possible  $m_F$  state collision combinations, that the magnetic field is not set too far from its optimum value, that the non-optically pumped gas components  $m_F$  state populations are rebalanced frequently enough that they do not stray too far from their average values, that the temperature of the two components is approximately equal at all times, and that the gases are in kinetic thermal equilibrium. Finally, it is assumed that the gases are confined in a harmonic potential. Using these reasonable assumptions and detailed balance considerations, the predicted 2-CAZ cooling rate is given by equation (1) in the executive summary sections, and is repeated here for convenience:

$$\frac{dT}{dt} = -\frac{1}{\tau_{SE}} \frac{\exp\left(\frac{-\Delta}{k_B T}\right) N_2}{3k_B (N_1 + N_2)} (\Delta - \kappa) \frac{1}{1 + \tau_{OP} / \tau_{SE} \left(1 + \exp\left(\frac{-\Delta}{k_B T}\right)\right)} \quad (1)$$

where again  $T$  is the temperature of the gas,  $\Delta$  is equal to  $\mu_B/6$ ,  $\kappa$  is the amount of heat imparted per successful optical pumping event,  $k_B$  is Boltzmann's constant,  $N_1$  and  $N_2$  are the number of non-optically pumped and optically-pumped atoms respectively,  $\tau_{SE}$  is the spin-exchange collision rate time constant determined from the average density of the  $N_1$  atoms and the weighted spin-exchange collision rate given the average state  $m_F$  populations, and  $\tau_{OP}$  is the characteristic time it takes to successfully optically pump an atom to its desired state.

The comparison of the predicted cooling rate in equation (1) to the cooling rate measured experimentally was one of the primary goals of the work represented in our recent submitted publication. If equation (1) is a reasonable description of the achievable cooling rate, then it can be used to estimate the performance of 2-CAZ cooling for other atom combinations and for other experimental conditions. Another goal of the experiment was to characterize the unavoidable heating term  $\kappa$  in an actual implementation of the cooling (as opposed to a theoretically considered one). The value of  $\kappa$  sets a lower limit on the lowest realistically achievable temperatures that could be obtained with this cooling method.

#### IV.D Experimental Measurements

The details of our experimental apparatus are described in detail in the publication cited at the beginning of this section. In brief,  $^{85}\text{Rb}$  and  $^{87}\text{Rb}$  atoms were cooled and confined in a pair of overlapping MOTs. A 75W  $\text{CO}_2$  laser beam was used to create an optical trap in the region of space occupied by the MOTs. The MOT laser detunings and intensities were manipulated to load both isotopes of Rb into the optical trap simultaneously. Once in the trap, an external magnetic field was applied with a typical magnitude of 2 Gauss. We had the capability of applying laser light with a variety of polarizations and frequencies near  $^{85}\text{Rb}$  resonances to optically pump those atoms. We also could apply microwaves resonant with the  $^{85}\text{Rb}$  ground state hyperfine splitting. These microwaves could be used as part of an optical pumping



scheme, but also allowed us to measure the individual  $m_F$  state populations in the  $^{85}\text{Rb}$  component of the gas. To periodically rebalance the  $^{87}\text{Rb}$   $m_F$  state populations, rf is applied to the atoms through a set of 10-turn coils located inside the vacuum system above them. The rf is tuned to the  $^{87}\text{Rb}$   $\Delta m_F = \pm 1$  resonant frequency (1.39 MHz at 2 Gauss). The atom number and temperature is determined through standard absorption imaging.

For the majority of our data, we used an optical pumping scheme that involved the use of microwaves to drive transitions from the  $^{85}\text{Rb}$   $F=2$ ,  $m_F=-1$  state to the  $F=3$ ,  $m_F=-1$  state. The reason for this is that we found that even low intensity ( $12.1 \mu\text{W}/\text{cm}^2$ ) laser light resonant with the  $F=2$  state resulted in unacceptably large light-assisted collision loss rates ( $1.5 \cdot 10^{-12} \text{ cm}^3/\text{s}$ ). While the microwaves eliminated this loss channel, the optical pumping rate was then limited by the achievable microwave power that could be supplied to the atoms.

The most straightforward way to measure the 2-CAZ cooling rate would have been to eliminate any other heating and cooling rates, apply the 2-CAZ cooling, and measure the temperature of the gas as a function of time. Unfortunately, the simultaneous  $^{85/87}\text{Rb}$  loading physics described in section III above complicated such direct measurement of the cooling rate. The interference in simultaneous loading resulted in lower initial densities than were originally expected. This had two consequences. First, while the characteristic spin-exchange timescale was faster than the 5 second optical trap lifetime, it was not sufficiently faster than that to get into a regime where the CAZ cooling rate would exhibit runaway behavior and increase as a function of time.

Second, once the Rb atoms were loaded into the optical trap, their initial temperature was not low enough to avoid evaporation. The presence of evaporative cooling masks the effect of 2-CAZ cooling. The reason for this is that applying non-evaporative cooling results in smaller evaporative cooling rate thus the overall cooling rate changes by less than what would be expected from 2-CAZ cooling alone. See arXiv:1302.5035 for details.

Given this complication, we used an alternative technique to measure the 2-CAZ cooling rate. The 2-CAZ cooling was applied for multiple optical pumping cycles to let the gas come to a steady-state cooling rate. At this point, the population in the  $^{85}\text{Rb}$   $F=2$ ,  $m_F=-1$  state was

measured at a particular point in the 2-CAZ cooling cycle. By combining the measurement of the population with a characterization of the optical pumping efficiency (i.e. the fraction of  $^{85}\text{Rb}$  atoms were moved from the  $F=2, m_F=-1$  state to the  $F=2, m_F=-2$  state in a single optical pumping cycle) the amount of Zeeman energy removed from the cloud in an 2-CAZ cooling cycle could be determined since the magnitude of the externally applied magnetic field was known.

We term the Zeeman energy removed per unit time as the “maximum cooling rate” for our experimental parameters since the cooling cannot exceed the rate of energy removal from the gas. For our experimental conditions, after allowing time for the 2-CAZ to settle into steady-state operation, we measured at maximum cooling rate of  $10.50(71) \mu\text{K/sec}$  for typical experimental conditions. This can be compared to the prediction for these conditions that would be obtained from equation (1). To get the maximum cooling rate from equation (1), the parameter  $\kappa$  is set to be zero. Equation (1) predicts a maximum cooling rate of  $11.55 \pm 1.96 \mu\text{K/sec}$ , in agreement with our observations.

In order to get the net cooling rate, the heating introduced per successful optical pumping cycle ( $\kappa$ ) must be determined. There are several potential sources of such heat. Optical pumping requires spontaneous scattered photons, and the resulting random momentum kicks will heat the atoms in the gas. This heating can be compounded if the gas being pumped is optically thick as each spontaneously scattered photon will then scatter multiple times on the way out of the gas, imparting a random momentum kick each time. In addition, density-dependent collisions can also result in heating in addition to inducing loss.

By conducting auxiliary experiments, we were able to measure the heating imparted due to the optical pumping. We observed three primary sources of heat: spontaneous photons scattered during the optical pumping process, hyperfine-changing collisions while the  $^{85}\text{Rb}$  atoms were in the  $F=3$  state, and exothermic spin-exchange collisions while the  $^{85}\text{Rb}$  atoms were in the  $F=3$  state. Each of these components contributed about the same amount of heating and the total heating rate for our conditions was  $4.28(65) \mu\text{K/sec}$ . This results in a net cooling rate of  $6.22(97) \mu\text{K/sec}$ . We can convert the measured heating rates determined above to a value for

$\kappa$  through using the cycle length, optical pumping efficiency, and relative number of  $^{85}\text{Rb}$  and  $^{87}\text{Rb}$  atoms such that  $\kappa/k_B=9.29\pm1.6\text{ }\mu\text{K}$ .

#### IV.E Implications for Effective 2-CAZ Cooling

Initially, the goal of implementing 2-CAZ cooling was to cool the gas to  $\mu\text{K}$  temperatures without requiring the loss of atoms as part of the cooling process. This was not achieved in the  $^{85/87}\text{Rb}$  mixture in our system. In part, this was due to the difficulties in the simultaneous loading of the two isotopes. If this were the only problem, it could be addressed through improving the initial trap conditions through changes in the trap geometry, using hybrid magnetic/optical trapping, or using a pre-cooling technique to improve the cooling starting conditions. We have developed and done preliminary testing on a simple pre-cooling technique described in section VII.E below. Lengthening the background lifetime would be another way to address the initially low spin-exchange rate given the achievable loading parameters, at the expense of a substantial redesign of the experimental apparatus and a good deal of additional complexity. The pre-cooling technique should accomplish the same goals in a simpler fashion.

The simultaneous loading issues are the only limitation to effective cooling in this system, however. The measured value of  $\kappa$  presents an approximate lower limit to the practically achievable temperature using this technique. Thus, to get effective cooling to few  $\mu\text{K}$  temperatures, the value of  $\kappa$  would have to be improved (lowered) from its current value. While changes to the optical pumping beam geometry and replacing the microwave with a pair of beams to drive Raman transitions (to improve the optical pumping success rate) could improve  $\kappa$  by a factor of 2 with extensive modifications to the 2-CAZ apparatus, the heating occurring as a result of hyperfine-changing collisions is more problematic since it is density-dependent. Assuming the other difficulties with this implementation of 2-CAZ were addressed, the hyperfine-changing collision heating rate will increase with the increasing density in the gas as it cooled, becoming more problematic as the temperature of the gas was lowered. Alternatively, it would limit the achievable density and thus phase space density of the gas being cooled.

While this means that 2-CAZ cooling would likely be limited in an  $^{85/87}\text{Rb}$  mixture, 2-CAZ is flexible enough that atoms without hyperfine structure can be used in the cooling (unlike in CAZ cooling). Our results suggest that the ability to avoid hyperfine-changing collisions is an important consideration in evaluating the likely effectiveness of implementing this cooling technique between a given pair of types of atoms. Atoms such without hyperfine structure (e.g.  $^{52}\text{Cr}$ ) would thus be well-suited to serve as the atom being optically pumped in 2-CAZ. The only requirement besides a suitable spin-exchange rate would be that the two atoms in 2-CAZ have different g-factors in their ground states in order to take advantage of the linear Zeeman shift.

#### IV.F Multiple- vs. single-type-of-atom cooling

While the behavior of the  $^{85/87}\text{Rb}$  system prevented achieving low enough temperatures such that reabsorption began to limit the cooling, in other systems (ideally without hyperfine structure) the 2-CAZ cooling has promise for mitigating reabsorption as compared to one-isotope cooling techniques. Reabsorption has been a major limiting factor in light-based cooling schemes [25,26,39] and so its mitigation has promise for extending cooling schemes to lower temperatures.

The role of two different types of atoms in the reabsorption mitigation was discussed in the publication associated with this work. Because  $\Delta$  is a function of the externally applied magnetic field, its value can be optimized for a particular set of densities at a given temperature. In the limit where  $\tau_{\text{OP}}=0$  (fast optical pumping), the cooling rate is optimized for  $\Delta=k_B T + \kappa$ . In the limit that reabsorption is the dominant contribution to  $\kappa$ ,  $\kappa$  can be written as  $\alpha N_2$  where  $\alpha$  is a constant. It will be optimal to have  $N_2$  smaller than  $N_1$  in this case, and so equation (3) can be expressed in the limit that  $N_2 \ll N_1$  as

$$\frac{dT_{\text{opt}}}{dt} = -k_2 \frac{\exp\left(-1 - \frac{\alpha N_2}{k_B T}\right) N_2}{3V} T \quad (4)$$

where  $V$  is the effective volume of the gas such that the average density of  $N_2$ -type atoms is equal to  $N_2/V$ . The constant  $k_2$  is the appropriately weighted spin-exchange rate constant. Equation (4) has an optimum at  $N_2 = k_B T / \alpha$ . Thus, if  $N_2$  is greater than this value, the cooling rate is increased if the number of atoms  $N_2$  is decreased. Reducing the optical thickness of the gas being optically pumped can thus increase the cooling rate even at the expense of a reduction in the number of spin-exchange events occurring per second.

This optimization can result in orders-of-magnitude increase in the achievable cooling rate as compared to the single-isotope cooling rate.  $N_2$  has to be able to be reduced to a chosen level, but that is often possible through using on-resonant beams to push  $N_2$  atoms out of the optical trap. Figure 3 compares the single-type-of-atom and optimized two-types-of-atoms cooling rates in the limit that the optical pumping heating is due to reabsorption.

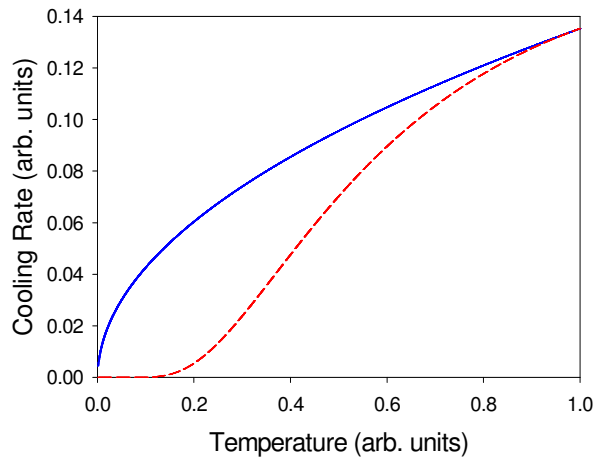


Figure 3. Relative performance of CAZ vs. 2-CAZ cooling. The blue solid line corresponds to the 2-CAZ case where the number of optically pumped atoms ( $N_2$ ) is continually optimized to produce the fastest cooling while the red dashed line corresponds to not having the ability to adjust  $N_2$ . The plot is for comparison and so the units are arbitrary. It is assumed that the dominant heating is proportional to  $N_2$  through reabsorption and so equation (4) determines the cooling rate. Note the very large relative cooling rate differences at  $T < 0.2$ .

In a more suitable system for 2-CAZ cooling, the two-atom nature of the cooling may produce strong benefits for extending non-evaporative cooling techniques to lower temperatures than those observed in single-atom non-evaporative cooling measurements.

## V. Enhanced two-color light-assisted collisional losses in Rb MOT

*Publication:* T. M. Wilson and J. L. Roberts, *Enhanced light-assisted-collision rate via excitation to the long-lived  $5S_{1/2}$ - $5D_{5/2}$  molecular potential in an  $^{85}\text{Rb}$  magneto-optical trap*, Phys. Rev. A **83**, 033419 (2011)

Multiple aspects of our experimental apparatus and research directions made it straightforward to investigate physics that was reported by Brett DePaola's research group at Kansas State University [40,41] in which they explored novel photoassociative ionization processes in a Rb MOT via ladder excitation. Through communication with the KSU group, we learned that adding light that resonantly drove transitions from the  $5P_{3/2}$  state (the first excited state and the state to which the laser cooling light couples the ground state) to a more highly excited  $4D_{5/2}$  state resulted in extraordinarily fast loss from the MOT. It was unknown whether that loss was due to the photoassociative ionization processes that they were studying, some disruption of MOT loading, or due to some other mechanism. We examined a similar experimental situation in order to try to gain insight as to what the mechanism for this loss was.

Our motivations for studying this loss went beyond simply wanting to determine the loss mechanism. While the KSU work focused on the photoassociative ionization physics itself, we were interested in the end products. Specifically, one of the results of the photoassociative ionization process was a highly excited molecule and a free electron. Given the ability of optical trapping and, in principle, 2-CAZ cooling to create highly compact, very dense atomic gases this photoassociative ionization could potentially be used to create an ultracold neutral plasma in a novel way. Not only could this be a useful system in which to study different aspects of ultracold neutral plasmas, it would enable their creation without needing a pulsed photoionizing laser. In order for such a plasma creation scheme to be viable, however, there were two requirements: the light-assisted collision rate had to be fast enough – at least  $10^{-10} \text{ cm}^3/\text{s}$  for the densities and atom numbers that we predicted that we could produce, and the extraordinarily fast loss from the MOT needed to be mostly due to the photoassociation process. Our measurements were consistent with the first requirement being met, but not the second.

Our apparatus was well-suited to this measurement because of the need to have overlapping MOTs in order to simultaneously load  $^{87}\text{Rb}$  and  $^{85}\text{Rb}$  into the optical trap. This meant that there were beams paths available that enabled two different frequency laser beams to uniformly illuminate the same volume of space in the vacuum apparatus. Our studies of light-assisted collision loss in optical traps also meant that we had developed a wide range of analysis tools to measure such a loss rate and meant that we had experience with the difficulties that can be encountered in such measurements.

To examine the nature of the physics that could be involved in the highly enhanced loss observed at KSU, we illuminated an  $^{85}\text{Rb}$  MOT with light that coupled the  $5\text{P}_{3/2}$  state to the  $5\text{D}_{5/2}$  state, a more highly excited state than Ref. [40,41]. This was primarily done for convenience – the wavelength of the  $5\text{P}_{3/2}$  to  $5\text{D}_{5/2}$  transition is 776 nm, close enough that we could pull our diode lasers that normally operated at 780nm to excite the desired transition. The photoassociation via ladder excitation would be significantly different in for the  $5\text{D}_{5/2}$  case because of its substantially larger energy. Thus, any significant difference in response that we observed could indicate the role that ladder excitation played in the overall loss.

However, our very first observations were qualitatively similar to those reported from KSU. When the MOT was illuminated with the 776nm light, there was an extraordinarily fast loss that occurred. The task we then set ourselves was to discover the cause of the loss and then see if it was likely to be present on other transitions as well.

The experimental details are presented in the publication cited above. Briefly, an  $^{85}\text{Rb}$  MOT was created using standard techniques and allowed to load from the background Rb vapor. This MOT was then illuminated with light resonant with the  $5\text{P}_{3/2}$  to  $5\text{D}_{5/2}$  transition. This light was coupled via a non-polarizing beam splitting cube onto the MOT light paths and thus illuminated the atoms from all six directions in an approximately balanced way. Once the additional light was on, the MOT fluorescence was observed to decay with time. Additional tests showed that this decrease was due to additional losses in the MOT, and not to a reduction in the MOT loading rate or a change in the 780nm photon scattering rate due to the  $5\text{P}_{3/2}$  to  $5\text{D}_{5/2}$  light. The decrease in fluorescence could thus be fit to a density-dependent loss model, and the loss rate induced by the  $5\text{P}_{3/2}$  to  $5\text{D}_{5/2}$  light measured. Any volume changes in the MOT during the measurement were recorded by taking fluorescence images of the MOT with a CCD camera.

The shape of the atom-loss curves was used to establish that the observed atom loss was density-dependent and a number and a size calibration was performed to extract the loss rate itself for a given set of experimental parameters. To determine the origin of the loss, the variation of the loss rate with the intensity of the lasers involved (L1:  $5\text{S}_{1/2}$  to  $5\text{P}_{3/2}$ -resonant laser, used for laser cooling and L2:  $5\text{P}_{3/2}$  to  $5\text{D}_{5/2}$ -resonant laser used in induce the rapid loss) was measured. In the absence of saturation, the scaling of the loss rate with laser power indicates the number of photons required for the induced loss. For instance, if the loss rate were to scale linearly with L1, that would indicate that one L1 photon was involved in creating the loss. A variety of experimental techniques were used to extract the intensity dependences on the two lasers, and it was determined that the loss rate scaled linearly with both lasers.

The fact that one L1 and one L2 photon were involved in creating the loss indicated that the loss channel was associated with a molecular potential associated asymptotically with the  $5S_{1/2}$ - $5D_{5/2}$  state combination<sup>1</sup>. The energy of this state is such that it cannot couple to any  $Rb_2^+$  states at any internuclear separation, and thus photoassociative ionization was not responsible for the loss. The interatomic forces associated with this state at long range are small compared to other possible state combinations, and so our observations were consistent with the loss occurring along a relatively “flat” intermolecular potential. This initially seemed problematic given the usual loss mechanism of radiative escape since there was relatively little acceleration of the atoms toward one another along the  $5S_{1/2}$ - $5D_{5/2}$  molecular potential. By examining the loss rate dependence on laser detuning, however, we observed that the maximum loss rate was associated with the atoms acquiring an initial acceleration towards one another along the  $5S_{1/2}$ - $5P_{3/2}$  molecular state before being excited to the  $5S_{1/2}$ - $5D_{5/2}$  potential. Further calculations showed that our observed losses were consistent with the atoms being accelerated towards one another on the  $5S_{1/2}$ - $5P_{3/2}$  molecular potential, then being excited to the relatively long-lived  $5S_{1/2}$ - $5D_{5/2}$  state where they could continue to approach one another, and then either decaying to the  $5S_{1/2}$ - $5P_{3/2}$  intermolecular potential via a spontaneous photon or undergoing a state-changing collision at short range. Since the atoms were able to travel closer to one another, the forces on the  $5S_{1/2}$ - $5P_{3/2}$  molecular potential could cause loss since their magnitude increases rapidly with decreasing internuclear separation.

The loss mechanism we associated with our observations would be expected to apply to a wide variety of states. In particular, it serves as a likely mechanism for the loss induced by  $5P_{3/2}$  to  $4D_{5/2}$  resonant light applied to a Rb MOT. The general implication of this result is that working with more highly excited states than the first excited state in a MOT can easily lead to loss for many different experimental parameters for many different atomic excited states. Knowing the loss mechanism allows for better selection of more favorable atoms and states for any experiments involving such more highly excited atoms. For instance, the narrow line cooling on excited states beyond the first excited state used in recent experiments in Li [8] would not be expected to have this type of associated loss since there are no long-lived states below the 3P state in Li. K [9] does have such long-lived states and exhibits a similar loss rate to the one that we report in Rb. An additional implication of our work is that in situations where such losses are present, a rapid MOT loading rate and relatively high pressure will be advantageous in mitigating the effect of these losses [10].

---

<sup>1</sup> From here forward the molecular states will be referred to by the asymptotic states of the atoms at large separation associated with the state in question



For our particular research program, this work was beneficial not only from the knowledge gained but from the impetus that it provided for us to investigate new directions in ultracold neutral plasma physics. A description of that direction of research is presented in the next section.

## **VI. A trap for ultracold neutral plasmas**

Through DURIP funding (FA 9550-09-1-0385) from the AFOSR, we were able to pursue the ideas that we developed about ultracold neutral plasma experiments through the assembly of a new experimental apparatus: a Penning trap for the confinement of ultracold neutral plasmas (UCPs). This apparatus should allow a significant extension of the useful lifetime of UCPs that should enable longer-timescale UCP physics phenomena to be studied. In particular, the goal of the research program is to study ion-ion and ion-electron thermalization processes in UCPs at cold enough temperatures that influences of strong-coupling plasma physics are relevant.

UCPs are created through the photoionization of a cloud of ultracold atoms. With typical sizes of  $\sim 0.5\text{mm}$  and densities of  $10^7\text{-}10^{10}\text{ cm}^{-3}$ , the initial electron temperature of these plasmas can be made to be as low as a few Kelvin with initial ion temperatures of a few mK. Despite these low temperatures, the ionization fraction of the initial atom cloud can be quite substantial. Thus, it is possible to create a highly ionized, yet very cold, plasma for studies of fundamental plasma physics. While multiple processes rapidly increase the ion and electron temperature after formation, these UCPs remain exceptionally cold for a two-component (i.e. ions and electrons) laboratory plasma.

The design of this apparatus is significantly different from other UCP experimental apparatuses in that the laser cooling and trapping is conducted in a different region of the vacuum system than where the UCP experiments are performed. While this adds additional experimental complexity, it frees the design of the plasma region from the constraints of needing to perform laser cooling and trapping there. For example, laser cooling performs best with ample optical access and a relatively large volume to accommodate  $\sim 1\text{cm}$  diameter laser beams. However, this requirement makes producing large magnetic fields problematic as smaller coils, for instance, are able to produce much larger fields for far less resistive power dissipation. As another example, even mildly sophisticated electrode design is problematic given the optical access requirements for laser cooling.

In our system, we are able to use segmented electrodes to apply a variety of electric potential configurations to the plasma. We are able to apply magnetic fields of up to  $\sim 0.1\text{T}$ . We have minimal requirements for optical access, needing only paths for two  $\sim 3\text{mm}$  diameter beams to photoionize the

atoms. Our ability to produce reasonably large magnetic fields and create a variety of electric potential configurations should allow for the confinement of UCPs in a Penning trap.

To obtain laser cooled atoms for photoionization in the UCP region of the apparatus, an  $^{85}\text{Rb}$  MOT is created in a different part of the vacuum system. Once the MOT has been loaded, the ultracold atoms are then loaded into a magnetic trap. This magnetic trap is physically transported along a track to move the atoms from the MOT region of the vacuum system to the UCP region of the vacuum system. This technique of transporting ultracold atoms has been used in the creation of Bose-Einstein condensates at JILA and elsewhere [42]. Once the atoms have been transported, the magnetic trap is turned off, and the atoms are photoionized to produce a UCP.

The design of the Penning trap for our system will be described in the next section. While trapping UCPs is a clear goal of our research, we have discovered interesting UCP behavior in our apparatus even at low values of or even zero magnetic field. In the course of the loading and the transport of our ultracold atoms, the rms size of the atom cloud in one direction increases to about 1.0mm (the cloud itself is approximately spherical). The number of atoms that we ionize can be made to be quite low, and so we are able to produce UCPs with much lower densities ( $\sim 10^7 \text{ cm}^{-3}$ ) as compared to other UCP systems. We have discovered that these lower densities have important implications for the UCP behavior. Collision times become longer. Thus, processes that are unobservable, or at least difficult to observe, in other systems because they have too short a timescale become more readily observable in our system. Likewise, collisional damping times become longer and so excitations of UCP motion are more persistent in our UCPs. In ongoing studies, we observe that evaporative cooling plays a significant role in the UCP evolution. The observation of significant evaporative cooling is promising from the perspective of trying to deliberately create UCPs with even colder electron temperatures. Three-body recombination is a major limitation to achieving lower temperatures in UCPs, but because of its strong density dependence it is almost absent in our system except at the very lowest electron temperatures. Finally, we observe short time UCP expansion behavior in a magnetic field that suggests interesting physics is occurring that we will need to understand in order to effectively load the Penning trap with a UCP at the coldest possible temperatures.

Several of these studies are ongoing, and will be briefly detailed below. After providing an overview of the design for a Penning trap in our system, I will summarize the results from our studies of UCP response to short electric field pulses and few-cycle rf pulses that have been published in Physical Review A. I will then present an outlook for future studies.

## VI.A Axial confinement of UCPs in a Penning trap

The confinement of UCPs in a Penning trap was demonstrated at the University of Michigan in Georg Raithel's research group [43]. In that trap,  $\mathbf{E} \times \mathbf{B}$  drifts were possible that limited the lifetime of the UCPs in the Penning trap. In our trap, we have taken care to preclude the possibility for ion and electron escape in that way. This section provides an overview of the design capabilities of our apparatus.

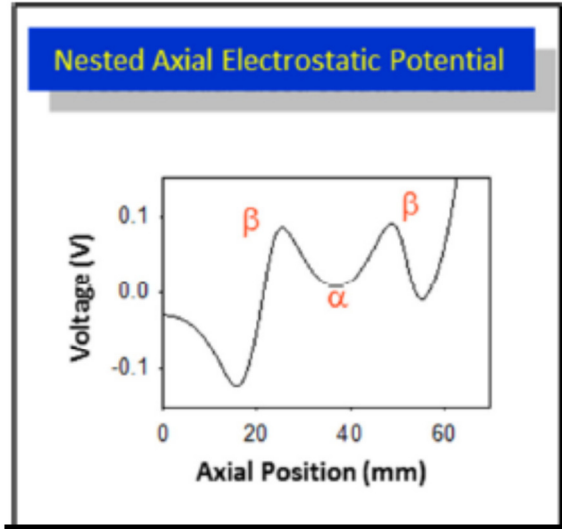
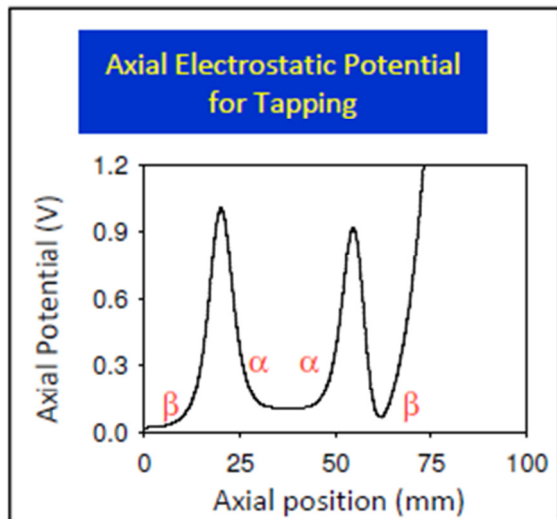


Figure 4. Nested Penning trap axial potential. This figure shows the structure of the Penning trap potential in the axial direction when charged particles of different signs are to be trapped. Ions will be trapped at the point  $\alpha$  and electrons at the points  $\beta$ .

In a Penning trap, charged particles are confined radially by a strong axial magnetic field. For either positive or negative charges, any motion initially away from the center of the trap in a radial direction will result in a Larmor orbit, and thus the radial extent of the motion of the particles will be limited. For confinement in the axial direction, electrostatic potentials are used. While this is fairly straightforward for particles with only a single sign of charge being confined, if particles with different charges are to be confined this becomes more complicated. The reason for this is that a potential minimum for a positively charged particle is a potential maximum for a negatively charged one, and vice versa.



One possible way to confine both negative and positive charges is through the use of a “nested” Penning trap as is employed in the trapping of anti-hydrogen [44,45,46] and in [43]. The general shape of such an axial confining potential is shown in figure 4. In general, the opposite-signed particles

will separate in this trap, but as long as the effective temperature of the particles is greater than the barrier between the positive and negative particle trapping region, particles with higher thermal energy will transit the region where the oppositely charged particles are trapped, giving the particles a chance to interact.

Figure 5. The “standard” axial potential in which we plan to trap UCPs. Radial confinement is to be provided by a 0.1T magnetic field.

Such a situation is not ideal for a UCP where a goal is the study of plasmas with low temperatures. Instead, we plan to use a variation of the nested potential as shown in figure 5. In this potential, the UCP is created in the “flat” central region that is approximately free of any electrostatic forces. This allows the UCP to evolve without undue influence from external fields. The ions are confined to this central region by the increase in the potential shown at  $\alpha$  in figure 5. The electrons will be accelerated outward at this point, but they will reflect off the “outer walls” of the potential and return to the center.

There will be a tendency of the electrons to find their potential minimum at the relatively sharp local maxima in the electrostatic potential, and if the electrons collect there they will no longer interact with the ions. However, it is difficult for the electrons to lose enough energy to become confined in those regions. There are several reasons for this. First, the electrons are accelerated strongly by the field as they pass point  $\beta$  in figure 5, and so they do not spend much time in the region of high electrostatic potential. Second, the increase in electron energy leads to a reduction in the collision cross section that is necessary to cause the electrons to equilibrate into their potential minimum because of the strong energy dependence of the Coulomb collision cross section. Third, the magnetic field will inhibit energy transfer from the axial to the radial directions. Fourth, the confining potential can be manipulated to release some of the electrons to create a space charge that confines most of the electrons in the UCP.

Estimates based on energy equipartition rates [47] for our trap parameters results in an estimated lifetime of 20ms for 5K electrons, a significant improvement over the typical 0.1ms lifetimes of a UCP.

Longer UCP lifetimes promise make possible measurements that are not easily performed in shorter timescale UCPs. For instance, ion-ion equilibration over a wide range of parameters and damping of ion acoustic waves should be observable. Electron evaporation holds promise for significantly cooling of the electrons in the trap and should allow access to a greater degree of strong-coupling physics. Most interestingly, realizing a 20ms lifetime would enable the study of electron-ion thermalization. Understanding this last problem in detail has the promise of improving plasma theory through being able to experimentally evaluate a theoretically difficult problem.

While the majority of the required apparatus for Penning trapping is in place, in order to effectively load the trap there are questions currently outstanding about UCP behavior that is highly relevant to efficient Penning trap loading. In particular, investigations of short-time UCP expansion in a magnetic field should yield insight about how best to load the Penning trap. In addition, we are developing diagnostics that will be useful in interpreting the results of future measurements. The next section details our recent work studying the effect of few-cycle rf pulses and short pairs of electric field pulses on UCPs. The following sections discuss ongoing and future measurements.

## **VI.B UCP density-dependent response to few-cycle rf pulses**

*Publication: Truman M. Wilson, Wei-Ting Chen, and Jacob L. Roberts, [Density-dependent response of an ultracold plasma to few-cycle radio-frequency pulses](#), Phys. Rev. A **87**, 013410 (2013).*

The density of a UCP is a critical parameter that is required to interpret almost any UCP experiment in a useful way, and thus a reliable technique to measure UCP density is an important capability for any UCP experimental apparatus. Almost since the first experiments with UCPs their densities have been measured by applying resonant rf pulses to the UCP to excite plasma oscillations. In a uniform plasma of infinite extent, these collective plasma oscillations' oscillation frequencies have well-defined and direct relationship to the plasma density. For UCPs, the plasma frequencies associated with the average density of the UCP fall in the radiofrequency (rf) range and UCPs show a response to applied rf fields in that frequency range. The UCPs' density is not uniform though, and so the standard results from plasma theory cannot be applied directly.

Moreover, while UCPs exhibit a clear response to rf fields applied in the appropriate frequency range, the collective oscillations are not observed directly. Instead, the UCP response is inferred through an increase in electron escape rate associated with the applied rf field. In most theoretical treatments, it is assumed that the increase in electron escape is due to heating of the electrons in the plasma from rf-induced electron motion. The electrons' motion during the oscillation is assumed to be converted into heat by randomizing electron-electron or electron-ion collisions.

The density of the UCP is not only an indispensable parameter that is one of the primary descriptions of the UCP. By combining the knowledge of the number of electrons in a UCP and its density, the size of the UCP can be extracted from density measurements. The change in size with time can then be used to measure the expansion rate of the UCP. Because the expansion rate is a function of electron temperature, information about the expansion rate also provides information on the temperature evolution of the electrons in the UCP during expansion.

In most experiments elsewhere, if rf was applied to the UCP while it expanded it was applied continuously. When this was done, a resonant UCP response would be observed at a particular time in the UCPs expansion. The interpretation of this observation was that the time of peak UCP response corresponded to the point at which the density of the UCP supported plasma oscillations frequencies equal to the driving rf frequency. By varying the rf frequency, the shift in the response time could be used to trace out the density of the UCP as a function of time.

In our recent experiments, instead of continuous rf we applied a short burst of rf, as few as two cycles of oscillation. The short timescale of the pulse made it easy to observe the delay between the application of the rf pulse and the response of the UCP. Density-dependent resonant behavior of the UCP was still observed. However, the timescale of the UCP response was too fast for collisions to have time to thermalize the plasma oscillation motion and produce energetic electrons required for the observed response signal. Thus, some other mechanism had to be responsible for the observed UCP signals.

We proceeded to make additional measurements of the UCP response to two-cycle rf pulses. We observed a clear resonance in the UCP response. The resonance was consistent with being density-dependent, and the extracted UCP size behaved as expected for an expanding UCP. We compared the peak frequency response of the UCP with two-cycle rf pulses to the UCP response to continuous rf, and found agreement as long as the power of the continuous rf was extrapolated to zero.

Further studies allowed us to identify the response as being due to the motion of the electron component of the UCP as a whole in response to the applied rf fields. We developed a simple model of the response by treating the electrons as a solid object and then calculating the frequency of oscillation of the center-of-mass motion of the electrons when they were displaced from the ions. For most of our UCP conditions, this model was very good at producing consistent peak density measurements for UCPs with different experimental parameters but the same peak density. For instance, the density obtained shortly after UCP formation before it had a chance to expand was consistent over different initial ionization energies. Electric field pulses were used to deliberately alter the charge imbalance of the UCP at a given time in its expansion and again the model produced consistent density predictions even as the resonant rf frequency shifted in response to the changing charge imbalance.

In order to theoretically investigate the mechanism for the UCP response, we calculated the motion of individual electrons in the macroscopic field caused by the displacement of the whole electron cloud with respect to the ions. When the electron cloud is displaced, an electric field is created that has the approximate form of a macroscopic dipole field, which in turn oscillates with the oscillating electron cloud. An electron moving in this field can experience gain a significant amount of energy from these fields for appropriate values of initial position and velocity. This energy increase comes about because there is a spatial variation in the induced electric field. An electron can be accelerated by the electric field for a time, but then move to a position where the field is smaller when the sign of the field reverses. In that case, energy will have been imparted to the electron by the oscillating motion of the whole electron cloud.

For energetic electrons in the thermal distribution of velocities that are close to escaping the UCP, this additional energy can drive them out of the UCP, producing the observed response. Quantitative estimates for our experimental parameters indicated that the induced fields were large enough to account for our observed signals.

This model predicted that this oscillating motion could be introduced not only with an rf pulse, but with a sharp (FWHM 12.5 ns) electric field pulse. We applied pairs of sharp electric field pulses and observed the UCP behavior. In response to both pulses, additional electrons escaped the UCP since the applied field accelerated them out of the UCP. By varying the delay time between the pair of pulses, we observed that the electron response to the second pulse oscillated with delay time, indicating an oscillation in the UCP (figure 6). The frequency of the oscillation set up by the first pulse matched the resonant rf response frequency that we measured for the same UCP conditions.

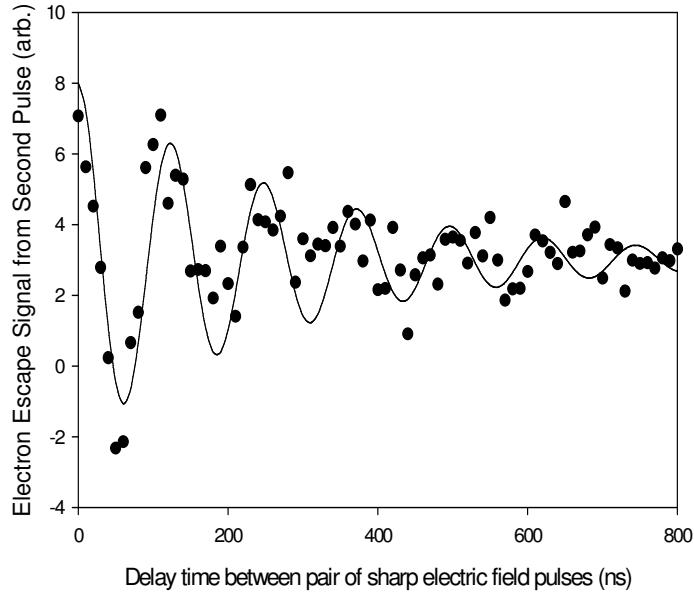


Figure 6. UCP oscillations induced by two sharp electric field pulses. The points on this figure correspond to the amount of electrons driven out by a second sharp electric field pulse applied a variable amount of time after a first sharp electric field pulse. Both pulses are oriented to drive electrons out of the UCP and toward the detector. The solid line is a damped sine wave fit to the data. Our interpretation is that the first pulse starts an oscillation of the electron cloud that then influences the electrons driven out by the second pulse. The frequency of the sine wave matches the resonant response frequency of short-pulse rf fields applied to the UCP.

There are several implications of these observations for future studies in our UCP system. First, in the absence of determining the mechanism for the resonant response, we would have not been able to correctly ascertain the density of the UCP. This was apparent from the data where we measured the rf response as a function of the deliberately altered charge imbalance. If we used the “typical” theory [13] rather than one that reflected our actual experimental conditions, then the resulting densities that we would have extracted would have been inconsistent. In other words, the theory of Ref. [13] does not correctly predict the size from the rf resonant response for the lower density UCPs that were the objects of study in our system.

Another implication of these results is that it is possible for electron motion to transfer energy in the UCP faster than would be implied by predicted electron thermalization rates. As we seek to measure electron thermalization, we have to be aware of this possibility to prevent it from distorting our results. Finally, the UCP oscillation as observed by applying two electric field pulses represents an unexpected tool that we now have to investigate UCP behavior.



## **VII. Investigations started during the reporting period, still in progress, and future work**

This section will summarize lines of investigation that were begun during the reporting period and are still in progress. After a brief description of the investigation is given, its current status will be reported.

### **VII.A Evaporative cooling in ultracold plasmas**

As has been mentioned in the previous two sections, our UCPs are larger and therefore have significantly lower densities than typical UCPs in other systems. One of the consequences of lower density is that evaporative cooling plays a much larger role in the UCP electron temperature evolutions and UCP expansion. For some sets of parameters, evaporative cooling is the dominant energy loss mechanism in our UCPs.

At first glance, this may seem to be a counter-intuitive result. Evaporation is driven by thermalizing collisions creating high-energy atoms in a thermal (and in our case close to Maxwell-Boltzmann) distribution. Since the collision rate scales linearly with the density, it might seem that increasing the density will increase the collision rate, which will in turn increase the evaporation rate, which will then result in more evaporative cooling.

The reason that this line of thinking does not apply to UCPs is because of the fact that the electron confinement is not from external, but is rather from internal fields. Thus, as electrons are lost the UCP confining potential becomes deeper due to an increase in the space charge. The deeper potential slows evaporative cooling, since the evaporation rate is proportional to  $\exp(-\eta)$ , where  $\eta$  is the ratio of the confining potential depth to  $k_B T_e$ , where  $T_e$  is the electron temperature. Thus, any increase in collision rate is quickly tempered by a drop in the evaporation rate due to the deepening potential.

We do observe an increasing absolute evaporation rate with increasing density obtained by ionizing more atoms. However, the resulting increase in evaporation rate and the concomitant increase in absolute energy removed per unit time are largely offset by the increase in the heat capacity of the electron gas. In other words, the increased level of absolute cooling that we observe as a result of a larger UCP density does not result in a strong change in the relative amount of cooling, and thus the temperature evolution of the electrons does not change rapidly with increasing number. We have developed a numerical model to examine this behavior and find that the model reproduces this aspect of the observed UCP behavior.

Using the two-cycle rf technique described in section VI.B above, we have measured the expansion rate of UCPs in our system as a function of time. We find that the expansion rate is less than what would be expected from the initial ionization energy imparted to the UCP. By examining the electron loss during the expansion, we find that the decrease in expansion is consistent with evaporative cooling influencing the UCP expansion. Changing the number of initially ionized atoms has a minimal impact, as suggested by our numerical model.

We have collected most of the necessary data for publication for this project. We are refining our models and investigating whether or not an applied electric field has an impact on the initial expansion energy in our system.

Slightly beyond the current scope of this study, we note that with the observation of significant evaporation in our ultracold plasmas, a natural question is whether or not even lower electron temperatures can be obtained through forced (i.e. deliberately increased) evaporative cooling. With lower densities, the primary heating mechanism of three-body recombination is much reduced, and simple estimates indicate that it should be possible to create higher values of the strong-coupling parameter  $\Gamma$ , at least for some time, in our low-density system than would otherwise be the case.

We can deliberately increase the evaporation rate from the UCP using an applied electric field. We can conduct measurements that are sensitive to the UCP size at the 3% or better level, and thus can look for changes in expansion rate due to changes in electron temperature as a result of applied pulses. We have already collected data that shows that we are sensitive to such alterations in the electric field in the opposite direction – that is we have showed that the expansion rate can be made to increase by reducing the evaporative cooling rate. For technical reasons, this is easier to observe than the opposite, but we plan to conduct measurements where the cooling is deliberately increased.

### **VII.B Magnetic field influence on initial ultracold plasma expansion rate**

The work described in this section is of a more preliminary nature than the work described in the previous subsection. Loading UCPs into a Penning trap will require creating the UCPs in a high magnetic field. When we apply a mild magnetic field to our atoms, however (approximately 1 mT), we see that the UCP expansion is altered significantly. Specifically, the expansion rate is much larger than in the magnetic-field-free case. The increased expansion rate appears to saturate at around 2 mT, but any

increased expansion rate could be problematic in Penning trap loading if it increases the initial energy of the ions. Thus, we are investigating the nature of the increased expansion rate.

To date, the onset of the increase in expansion seems to be correlated with a magnetic field strength that results in a predicted Larmor radius of the electrons to be on the order of the size of the UCP. Thus, it seems that this increased expansion is driven by a lack of mobility of the electrons in the UCP as they become “frozen” radially to the magnetic field lines. We have developed some simple numerical models that are consistent with this picture, and are discussing more sophisticated models with theoretical collaborators.

We plan to continue to collect data to characterize the nature of this effect. Variations in ion/electron number, initial ionization energy, magnetic field, and applied electrostatic potentials will be explored and should shed additional light on the source of the additional expansion rate. Where possible, comparisons between our experiments and theory will be conducted.

### **VII.C Ultracold plasma damping rate**

When we apply two separated electric field pulses to the plasma, not only do we observe oscillation but we also observe damping of the oscillation. This damping could have multiple sources, but one source should be electron-ion collisions that do not transfer energy but do change the direction of electron motion. Preliminary data indicate that the damping rate scales with the predicted electron-ion (and to a lesser extent electron-electron) collision rate – increasing with increasing density and decreasing with increasing temperature.

Our electron evaporation measurements provide constraints on the electron temperature shortly after the formation of the UCP. By studying the oscillation damping rate shortly after UCP formation, we can observe the relationship between the measured damping rate and the prediction electron-ion collision rate. By going to the highest possible temperatures and lowest possible densities, we can search for any damping rate component that persists even as the predicted collision rate goes to zero. This damping rate is an indication of the contributions from other non-collisional mechanisms to the damping. By studying the behavior of any observed component, we can attempt to account for it to isolate the electron-ion (and electron-electron) collisional component to the damping.

Such a measurement would be useful for comparison to numerical models of UCP behavior where the proper treatment of electron-ion collision is problematic due to the attractive nature of the Coulomb

interaction between these two different particles. Additionally, we can access parameter ranges where strong-coupling physics is expected to contribute to the value of the collision rate (although we cannot go deeply into the strong-coupling regime at this time) to study any influence that has on the extracted damping rate.

This work is also in preliminary stages and is quite data intensive. There are many open questions about the sources of the damping rate. Nevertheless, the scaling with predicted collision rate is qualitatively very apparent and we are hopeful that this investigation will produce fruitful measurements.

#### **VII.D Spin-exchange collision rate measurement**

While the previous three subsections are concerned with ongoing work with ultracold plasmas, there are two areas of research that were started during the project period that are also ongoing, but with Colorado State University support. The first area of study is the measurement of the spin-exchange collision rate in the optically trapped  $^{85}\text{Rb}$  and  $^{87}\text{Rb}$  mixture. The second area of study, covered in section VII.E below, is a relatively simple technique to enhance optical trap loading by cooling atoms shortly after they have been loaded into the optical trap.

Because of the experimental requirements of 2-CAZ cooling, that apparatus was capable of measuring the spin-exchange collision rate between  $^{85}\text{Rb}$  and  $^{87}\text{Rb}$ , which has not been reported in the literature. We proceeded to measure the spin-exchange rate, and are currently in communication with an atomic theorist about computing the expected relevant collision rates. Once predictions are available, they can be compared to experiment. At this point in time, for the data set we have we should be able to determine the average spin-exchange rate to 30% precision, including both systematic and statistical uncertainties. We expect to complete this work, which is no longer externally supported, in the next few months after discussions with our theory collaborators.

#### **VII.E Spatially-selective Hyperfine Pump Cooling**

As mentioned in section IV.D above, one of the factors that limited the performance of 2-CAZ cooling was the fact that the initial atom density was inhibited by cross-isotope optical trap loading interference between  $^{85}\text{Rb}$  and  $^{87}\text{Rb}$ . While it is difficult to avoid the simultaneous loading physics described in section III, once the atoms are loaded into the optical trap, in principle the density could be improved by modifying the optical trap geometry. Indeed, such a modification is performed in experimental systems elsewhere [48,49].

While we have the capability of performing such modifications of trap geometry and they were useful in creating more favorable initial density conditions, the performance was hindered by an excess of energy in the axial direction of our optical trap. Eventually, 2-CAZ and evaporative cooling removed this energy, but while it was present increasing the confining potential of the trap to increase the density of the atoms resulted in more heat imparted to the trapped atoms than would have otherwise been the case without this excess energy.

The excess energy originates because the optimal alignment of the optical trap with the MOT places the center of the optical trap offset from the center of the MOT [29]. This results in a larger optical trap volume at the atom location while still maintaining overall depth for the optical trap. As the atoms are cooled into the optical trap, however, this offset translates into additional axial energy.

The removal of this energy would result in a cooler and denser cloud of atoms in the optical trap. This would be useful not only for 2-CAZ cooling, but also as an improved starting point for evaporative cooling. In fact, it would be generally desirable for a wide variety of experiments with optically trapped atoms.

To this end, we have developed a very simple cooling scheme to rapidly remove the excess energy in the axial direction of the trap. This cooling scheme is laser-based, but requires no additional lasers beyond those already required for trapping and cooling the atoms in a MOT. The scheme promises to be robust with respect to magnetic field environment, atom density, and optical trap parameters. The only requirement is that the optical confining potential be non-spherical. That is easily satisfied in our elongated optical traps. This cooling scheme does require using atoms with ground state hyperfine structure.

Our initial implementation of this cooling scheme uses  $^{87}\text{Rb}$  atoms that are optically pumped into their lower hyperfine ground state ( $F=1$ ) after being loaded into the optical trap. The basic idea of the cooling scheme is to exploit the fact that atoms with higher axial energy than the average value in the gas will have larger axial orbits in the optical trap. The axial extent of the atoms shortly after loading is over 1.0mm in size in the axial direction. An optical pumping beam illuminates the outermost 15% of the atoms on one side of the trap for a selected pulse length to pump them into the  $F=2$  state. The light is then extinguished, and the atoms then move toward the center of the optical trap (on average) due to the confining potential.

Near the center of the trap the atoms are illuminated by a “stopping” laser pulse that consists of a beam near the cycling transition whose propagation direction is opposite of the atoms’ motion. Again a pulse is applied to the atoms, with the intent that multiple photon scatters will remove the center-of-mass motion of the atoms. Once this pulse is completed, the frequency of the stopping laser is altered and the atoms are pumped back down to the  $F=1$  state. The cycle can immediately begin again with atoms that have traveled to the edge of the optical trap.

Preliminary estimates for the effectiveness of this cooling are very positive. Cooling rates in excess of  $300\mu\text{K/s}$  should be possible, rapidly removing the excess energy and then actively cooling the axial motion of the atoms. Since on average the direction of the atoms’ motion is known, the cooling is very ‘efficient’ in its use of photons, as on average there will be no photons scatters in the “wrong” direction. This scheme is similar to Sisyphus schemes [50,51,52] that rely on optical pumping and confining potentials to create a closed cooling cycle, but those schemes do not use photon scattering to slow the atoms – the confining potential is used instead.

During the project period, we demonstrated that we could effectively optically pump the atoms in a spatially-selective way. We observed these atoms’ motion in the optical potential and can identify when they are at the optimal position to illuminated by the stopping laser. We have overlapped the stopping laser with the optical trap beam and exerted forces on the atoms, but we had to deal with a technical issue where loss-inducing light was “leaking” along an AOM deflection path. That has been rectified, and once personnel are available we will examine the cooling rate that can be achieved.

We plan to continue these measurements that were started during the project period with Colorado State University support. We are hopeful that we will observe cooling in the near future and be able to investigate the overall performance of this cooling technique.

## **VIII. Conclusion**

We implemented 2-CAZ cooling in an  $^{85}\text{Rb}/^{87}\text{Rb}$  gas mixture and were able to measure the achievable cooling rate and the heating rate during optical pumping for actual experimental conditions. The primary conclusion of this work is that the  $^{85}\text{Rb}/^{87}\text{Rb}$  system presents severe challenges for the 2-CAZ cooling technique. Partly this comes from unexpected physics in the simultaneous loading of the two isotopes into an optical trap, but more importantly the window is narrow to both avoid reabsorption by using low enough light intensities during optical pumping while still pumping the  $^{85}\text{Rb}$  atoms fast enough

out of the  $F=3$  state to avoid significant hyperfine-changing collision loss. The 2-CAZ technique still has theoretical promise in terms of mitigating reabsorption as compared to single-isotope cooling, but our research indicates that implementation will be much more favorable if the atom being optically pumped does not have hyperfine structure (e.g.  $^{52}\text{Cr}$ ).

The simultaneous loading of  $^{85}\text{Rb}$  and  $^{87}\text{Rb}$  from a MOT into an optical trap was investigated in detail. The need to address the unfavorable loading has led to a novel cooling technique that has great promise for being very efficient, very robust, and applicable to a wide variety of different situations beyond the studies associated with this project. While research into the effectiveness of this new technique is ongoing, so far all indications are positive.

As a by-product of the experimental requirements for studying 2-CAZ cooling, our apparatus was suited to measuring the spin-exchange collision rate between  $^{85}\text{Rb}$  and  $^{87}\text{Rb}$ , and also an extraordinarily fast loss created by illuminating an  $^{85}\text{Rb}$  MOT with light that coupled atoms in the first excited state to higher excited states.

This led in an indirect way to a new experimental apparatus for the study of ultracold neutral plasmas. We have constructed an apparatus capable of confining ultracold plasmas in a Penning trap. The medium-term goal of this research direction is to extend the lifetime of ultracold plasmas in order to investigate processes whose timescales are too long to study in expanding ultracold plasmas. By virtue of how a Penning trap works, we will also be examining ultracold plasma physics at relatively high magnetic field. Our initial focus is intended to be ion-ion thermalization, especially with electrons cold enough the strong-coupling physics is relevant, electron-ion thermalization, the general behavior of the ultracold plasma in the Penning trap (e.g. lifetime, heating rates, stability), and investigation of forced evaporative cooling.

After the construction of our apparatus, we observed that the density of the ultracold plasma created in our apparatus is much lower (by 1-2 orders of magnitude) than in other typical ultracold plasma experiments. This lower density turns out to be advantageous in many ways: collisional damping times are longer allowing the observation of oscillations and collisions processes that would be difficult to observe otherwise, evaporative cooling plays a significant role in the electron temperature evolution, and three-body recombination, which leads to loss and heating, is greatly reduced. We have studied the response of these lower density plasmas to short rf pulses and short electric field pulses and observed oscillations associated with the motion of the entire electron cloud. The damping of these oscillations

was also clear and may be a way to study electron-ion processes in an ultracold plasma before having to confine them to a Penning trap. We have also observed the expected increased role of evaporation in these ultracold plasmas and expect to submit that work for publication shortly. Finally, we have observed that even mild 0.10 mT fields result in significant modification of the ultracold plasma expansion behavior. The ultracold plasma physics that we have been able to access already in this new apparatus has been unexpected and valuable.

- 
- [1] G. Ferrari, *Eur. Phys. J. D* **13** 67-70 (2001)
  - [2] T.C. Killian *et al.*, *Phys. Rev. Lett.* **83**, 4776(1999)
  - [3] N. Kurti, F. N. H. Robinson, F. Simon, D. A. Spohr, *Nature* **178** 450 (1956)
  - [4] M. Fattori *et al.*, *Nature Physics* **2**, 765 (2006)
  - [5] Y. Castin, J.I. Cirac, and M. Lewenstein, *Phys. Rev. Lett.* **80** 5305 (1998)
  - [6] J. I. Cirac, M. Lewenstein, and P. Zoller, *Europhysics Letters* **35** 647 (1996)
  - [7] M. S. Hamilton, A. R. Gorges, and J. L. Roberts, *Phys. Rev. A* **79**, 013418 (2009)
  - [8] P. M. Duarte *et al.*, *Phys. Rev. A* **84**, 061406 (2011)
  - [9] D. C. McKay *et al.*, *Phys. Rev. A* **84**, 063420 (2011)
  - [10] S. J. Wu *et al.*, *Phys. Rev. Lett.* **103**, 173003 (2009)
  - [11] S. Kulin *et al.*, *Phys. Rev. Lett.* **85**, 318 (2000).
  - [12] K. A. Twedt and S. L. Rolston, *Phys. Rev. Lett.* **108**, 065003 (2012)
  - [13] A. Lyubonko, T. Pohl, and J. M. Rost, *New J. Phys.* **14**, 053039 (2012).
  - [14] T. W. Hansch and A. L. Schawlow, *Optics Communications* **13** 68 (1975)
  - [15] D. J. Wineland, W. M. Itano, *Phys. Rev. A* **20** 1521 (1979)
  - [16] S. Chu *et al.*, *Phys. Rev. Lett.* **55** 48 (1985)
  - [17] P. D. Lett *et al.*, *Phys. Rev. Lett.* **61** 169 (1988)
  - [18] J. Dalibard and C. Cohen-Tannoudji 1989, *J. Opt. Soc. Am. B* **6** 2023 (1989)
  - [19] M. H. Anderson *et al.*, *Science* **269** 198 (1995)
  - [20] K. B. Davis *et al.*, *Phys. Rev. Lett.* **75** 3969 (1995)
  - [21] B. DeMarco and D. S. Jin, *Science* **285** 1703 (1999)
  - [22] K. B. Davis, M.-O. Mewes, and W. Ketterle, *Applied Physics B: Lasers and Optics* **60**, 155 (1995)
  - [23] N. Masuhara, J. M. Doyle, J. C. Sandberg, D. Kleppner, and T. J. Greytak, *Phys. Rev. Lett.* **61**, 935 (1998)
  - [24] C. J. Myatt *et al.*, *Phys. Rev. Lett.* **78**, 586–589 (1997)
  - [25] H. Perrin, A. Kuhn, I. Bouchoule, T. Pfau, and C. Salomon, *Europhys. Lett.* **46** 141 (1999)
  - [26] A. J. Kerman, V. Vuletić, C. Chin, and S. Chu *Phys. Rev. Lett.* **84** 439 (2000)
  - [27] Price G N, Bannerman S T, Viering K, Narevicius E, and Raizen M G 2008 *Phys. Rev. Lett.* **100** 093004; Moler K, Weiss D S, Kasevich M, and Chu S 1992 *Phys. Rev A* **45** 342-348; Barrett M D, Sauer J A, and Chapman M S 2001 *Phys. Rev. Lett.* **87** 010404; Holland M J, DeMarco B and Jin D S 2000 *Phys. Rev. A* **61** 053610; Granade S R, Gehm M E, O'Hara K M, and Thomas J E 2002 *Phys. Rev. Lett.* **88** 120405; Monroe C, Meekhof D M, King B E, Jefferts S R, Itano W M, and Wineland D J 1995 *Phys. Rev. Lett.* **75** 40114014; Wolf S, Oliver S J, and Weiss D S 2000 *Phys. Rev. Lett.* **85** 4249-4252; Aspect A, Arimondo E, Kaiser R, Vansteenkiste N, and Cohen-Tannoudji C 1988 *Phys. Rev. Lett.* **61** 826-829; Boyer V, Lising L J, Rolston S L, and Phillips W D 2004 *Phys. Rev. A* **70** 043405; Petsas K I, Courtois J Y, and Grynberg G 1996 *Phys. Rev. A* **53** 2533-2538; Stecher H, Ritsch H, and Zoller P 1997 *Phys. Rev. A* **55** 545-551; Ivanov V S, Rozhdestvensky Y V, and Suominen K A 2012 *Phys. Rev. A* **85** 033422; Dunn J W, Blume D, Borca B, Granger B E, and Greene C H 2005 *Phys. Rev. A* **71** 033402; Colom'e-Tatch'e M, Klempt C, Santos L and Vekua T 2011 *New J. Phys.* **13** 113021
  - [28] P. Medley *et al.*, *Phys. Rev. Lett.* **106** 195301 (2011)
  - [29] S. J. M. Kuppens *et al.*, *Phys. Rev. A* **62**, 013406 (2000)
  - [30] K. M. O'Hara, *Phys. Rev. A* **63**, 043403 (2001)
  - [31] A. Mosk, *APPLIED PHYSICS B-LASERS AND OPTICS* **73**, 791 (2001)



- 
- [32] U. Schloder, Phys. Rev. A **66**, 061403 (2002)
  - [33] J. Weiner *et al.*, Rev. Mod. Phys. **71** 1-85 (1999)
  - [34] A. R. Gorges *et al.*, Phys. Rev. A **78**, 033420 (2008)
  - [35] Eite Teisinga, private communication
  - [36] K.-A. Suominen *et al.*, Phys. Rev. A **57**, 3724 (1998).
  - [37] M. Marinescu and H. R. Sadeghpour, Phys. Rev. A **59**, 390 (1999)
  - [38] S. Chang and V. Minogin, Phys. Reports 365, 65 (2002)
  - [39] S. Wolf, S. J. Olive, and D. S. Weiss, Phys. Rev. Lett. **85** 4249 (2000)
  - [40] M. L. Trachy, G. Veshapidze, M. H. Shah, H. U. Jang, and B. D. DePaola, Phys.Rev.Lett. **99**, 043003 (2007).
  - [41] G. Veshapidze, M. L. Trachy, H. U. Jang, C. W. Fehrenbach, and B. D. DePaola, Phys.Rev.A **76**, 051401(R) (2007)
  - [42] H. J. Lewandowski *et al.*, J. of Low Temp. Phys. **132** 309 (2003)
  - [43] J. H. Choi *et al.*, Phys. Rev. Lett. **100**, 175002 (2008)
  - [44] M. Amoretti *et al.*, Nature (London) **419**, 456 (2002)
  - [45] G. Gabrielse *et al.*, Phys. Rev. Lett. **89**, 213401 (2002).
  - [46] G. Gabrielse, S. L. Rolston, L. Haarsma, and W. Kells, Phys. Lett. A **129**, 38 (1988)
  - [47] M. E. Glinsky *et al.*, Phys. Fluids B **4**, 1156 (1992).
  - [48] T. Kinoshita, T. Wenger, D. S. Weiss, Phys. Rev. A **71**, 011602 (2005)
  - [49] T. Weber, J. Herbig, M. Mark, H.-C. Nagerl, and R. Grimm, Science **299**, 232 (2003)
  - [50] N. R. Newbury *et al.*, Phys. Rev. Lett. **74**, 2196 (1995)
  - [51] Vladyslav V. Ivanov and Subhadeep Gupta, Phys. Rev. A **84**, 063417 (2011)
  - [52] J. Janis, M. Banks, and N. P. Bigelow, Phys. Rev. A **71**, 013422 (2005)